Spanning Between Theory and Practice

Session Organizer: Hiroki TAMAI (Illinois Institute of Technology)

Plenary Lecture: Abstract, Slides and Video
Large shell structures for power generation technologies
Wilfried B. KRÄTZIG (Ruhr-University Bochum), Reinhard HARTE (University of Wuppertal), Ralf WÖRMANN (Krätzig & Partner)

Keynote Lecture
Numerical tools in structure optimization
William BAKER, Alessandro BEGHINI, Juan CARRION, Aaron MAZEIKA, Arkadiusz MAZUREK (Skidmore, Owings & Merrill LLP)*

Design process, detailing and examples of non-traditional structures
Christian STUTZKI, Hiroki TAMAI, Joshua BUCKHOLT (Illinois Institute of Technology)*

Opportunities and risks with free-form design
Hans SCHOBER, Stefan JUSTIZ, Kai KUERSCHNER (Schlaich Bergermann and Partner LP)*

Novel space frame system based on Golden Ratio, 5-fold symmetry, and the fractal HyperFrame system
Chris KLING, Hiroki TAMAI, Nicola D'SOUZA (Aurodyn, Inc.)*

Determination of warping deformation limits for insulating glass units in cable net facades
Hiroki TAMAI, Chris STUTZKI, Joshua BUCKHOLT, Mathew WEGLARZ (Stutzki Engineering, Inc.)*

Optimal design of unitized structures with curvilinear stiffeners
Rakesh K. KAPANIA, Pankaj JOSHI, Manav BHATIA, Thi DANG (VPI&SU)*

Buckling analysis of Wuhan Railway Station
Rongwei TANG, Pengfei ZHAO, Yong TAO, Guohua PAN, Jihong QIAN, Yixin DU (China Academy of Building Research)*

For multiple-author papers:
Contact author designated by *
Presenting author designated by underscore

Proceedings of the 6th International Conference on
Computation of Shell and Spatial Structures
IASS-IACM 2008: "Spanning Nano to Mega"
28-31 May 2008, Cornell University, Ithaca, NY, USA
John F. ABEL and J. Robert COOKE (eds.)

Large shell structures for power generation technologies

Wilfried B. KRÄTZIG*, Reinhard HARTE[1], Ralf WÖRMANN[2]

* Ruhr-University Bochum, Universitätsstrasse 150, D-44780 Bochum, wilfried.kraetzig@rub.de
[1] University of Wuppertal, Pauluskirchstrasse 7, D-42285 Wuppertal, harte@uni-wuppertal.de
[2] Krätzig & Partner Engg. Comp., Buscheyplatz 9-13, D-44801 Bochum, woermann@kraetzigundpartner.de

Abstract

In power generation industries large RC shell-like structures are well in use, as safety containments for LNG tanks, shafts for wind generators, smoke stacks, nuclear power plant containments, natural draft cooling towers, and in future solar upwind chimneys. Especially these last two types of shells form the largest shell structures in technology. Because of their size they are extremely exposed to storms and to seismic actions. Since attacked by environmental effects, the damage evolutions determine to a large extend their service-lives. Many structural phenomena, like forced vibrations, static and dynamic instabilities, or damage-induced failure, influence their safety and reliability. The present lecture will address some of these typical mechanical effects of large "wet" as well as "dry" natural draft cooling towers and for chimneys of solar upwind power plants.

1. "Wet" natural draft cooling towers

Due to the rising demand for cheap, economic as well as sustainable electricity, natural draft cooling towers (NDCT) at the "cold ends" of thermal power generation processes, have grown to enormous sizes and heights. Simultaneously, their shells developed to the largest reinforced concrete (RC) shell structures in technology. Compared to shell roofs or tanks, NDCTs are exposed on both faces to aggressive fuel combustion media. Additionally, aggressiveness in the towers' interiors is increased in Germany by release of cleaned flue gases therein, saving former customary smoke stacks (Krätzig *et al.* [3]).

So in addition to classical design conditions for load combinations of deadweight G, wind W, internal suction S, service temperature T, hygro-thermal attack H, and probably seismic actions E, durability is the key issue in the design of NDCTs. Possible structural shell repairs are limited to rather short shut-downs of the plant. Even in case of surfaces up to 60.000 m² each side for modern towers, sufficiently long shut-downs for careful surface repairs are illusionary.

The paper will report in detail on typical structural design efforts for cooling tower shells of extreme size, namely the shape optimization of the meridian, the construction of the flue gas inlet, the application of special acid-resistant high-performance concrete, and on design concepts to increase the shells' durability.

Here we describe the constituents of such huge wet NDCTs by example of the world-largest tower of 200 m of height at the RWE Power Station Niederaussem, some 20 km west of Cologne. Figure 1 shows the entire plant during construction in the year 2000. The new lignite power block BoA (left) has a net capacity of 965 MW, achieved by an efficiency of over 43%, the highest electrical net degree of efficiency of lignite fueled power plants worldwide. The 200 m cooling tower contributes considerably to this world record (Busch *et al.* [2]).

As confirmed in Figure 2, the total height of the cooling tower shell is 200 m. Its water basin diameter measures 152.54 m, that one of the lower shell rim 136.00 m, and the top opening is 88.41 m wide. Both the outer and inner shell faces measure about 60.000 m², equivalent to 10 soccer fields each. The tower shell is composed of two hyperbolic shells of revolution, meeting at the throat. It exhibits largely a wall thickness between 0.22 and 0.24 m, increasing towards the lower shell rim. The top edge of the shell is stiffened by an upper edge member with U-shaped cross-section, extending into the interior. The overhang measures 1.51 m with a shank-height of 1.20 m. To reduce crack-sensibility of the upper shell due to wind vibration, this edge member is pre-stressed by

Figure 1: Power Station Niederaussem (Photo RWE)

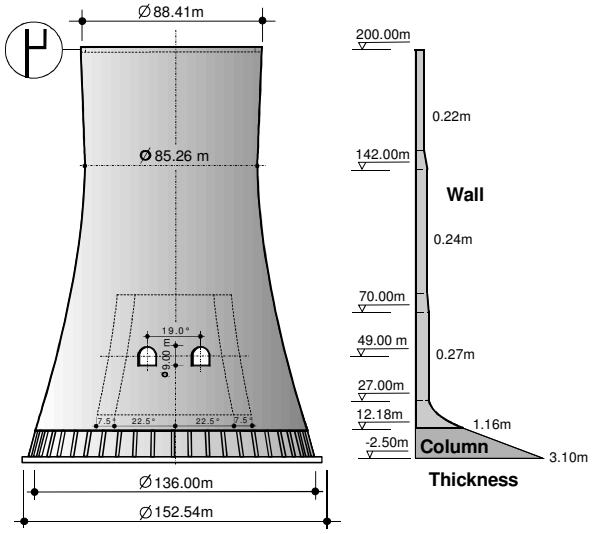

Figure 2: Dimensions of NDCT Niederaussem

4 SUSPA tendons with 8 mono-wires of 150 mm² cross-section each of steel quality St 1570/1770 N/mm². The lower edge member is formed by an increase of the shell thickness up to 1.16 m. The complete shell is made from acid-resistant high-performance concrete of compression strength of 85 N/mm², so-called ARHPC 35/85, to save a protective coating of the inner surface.

The cooling tower shell is supported by 48 meridional columns of 14.68 m of height, cast of RC 45/55 due to Eurocode EC 2. Their thickness ranges from 1.16 m on top to 3.10 m above foundation, their width is 1.40 m. All columns rest on a RC ring foundation of 6.60 m of width and 1.80 m of height. Softer soil than the standard consolidated gravel was exchanged. Along the water inlets and the water outlet the ring-width was enlarged.

All further tower components are conventional. The interior contains the water basin to collect the re-cooled water. Its basin plate and walls consist of water-proof RC 30/37 with 0.20 m of thickness, founded on a 0.15 m thick C 12/15 layer over an anti-freeze stratum of 0.30 m. The fill construction and the water distribution are designed as a prefabricated RC beam-column structure also made of high-performance concrete ARHPC 35/85.

The new Niederaussem power block BoA went into service in 2002, gaining excellent service experiences up to date. Presently, a series of new fossil fueled (lignite and hard coal) power stations is under design/construction in Germany since then, all with very similar NDCTs, and those common attributes mentioned at the beginning: Meridional shape optimization, cleaned flue gas release, ARHPC 35/85, design for durability. The lecture will present details of these attributes, and demonstrate design consequences of them, like preserving the original buckling safety, vibration properties and simulating the damage evolution over their life-times.

2. High "dry" cooling towers and low (mini) solar chimneys

Wet cooling systems consume cooling water through evaporation, as the vapor cloud above the tower indicates. If water consumption is unacceptable, "dry" cooling has to be chosen, in which the water is captured in a closed piping system. Then cooling works only by convection with lower efficiency, such that dry cooling towers have strongly enlarged dimensions. Already in the 1970ies large dry NDCTs were designed for power station in arid zones, reaching up to 300 m. With this height they approach low solar chimneys which start for professional operation at heights of approximately 500 m.

Figure 3 shows the design study of such a chimney. The tower has a total height of 500 m, diameters of 120 m at the throat and of 200 m at its base. The wall thickness increases from 0.25 m on the top to 0.60 m on the foundation slab. The shell with shape-optimized meridian requires a classical upper edge member and three intermediate stiffening rings. These stiffeners serve two important purposes,

- to reduce the buckling lengths of the shell for sufficient safety against instability failure,
- to constrain the meridional/shear forces in the shell due to wind towards a beam-like behavior.

The first purpose can be achieved with rather moderate sized cross-sections of all four stiffeners, attached on the shell outside, namely a hangover-width of 2.50 m and a thickness of 0.40 m. The second purpose requires stiffer rings in order to reduce the maximum wind tension towards the order of magnitude of the dead-load compression, an optimal design goal. With the above given dimensions, tension/shear stress maxima can be reduced up to 2/3. Higher reductions require internal spokes in the rings as recommended by (Schlaich *et al.* [4]).

Experienced designers of NDCT shells would attempt to construct the shell of Figure 3 without intermediate rings. The lecture will demonstrate for this case how the then globally extended instability modes require a thickness increase of the shell. Adding three sufficiently stiff intermediate rings, probably with spokes, as mentioned above lets the buckling safety of the shell grow by the factor 1.7.

3. Shells for future solar chimneys power plants

Due to Figure 4 Solar Chimney Power Plants (SCPP) consist of the glass-covered collector area, the turbo-generators for power conversion and the solar chimney. In the collector, solar radiation heats the collector ground and so warms up the enclosed air, which streams towards the center. There in the power conversion units, the energy of the air stream partly transforms into electric power, before being released through the chimney as pressure sink.

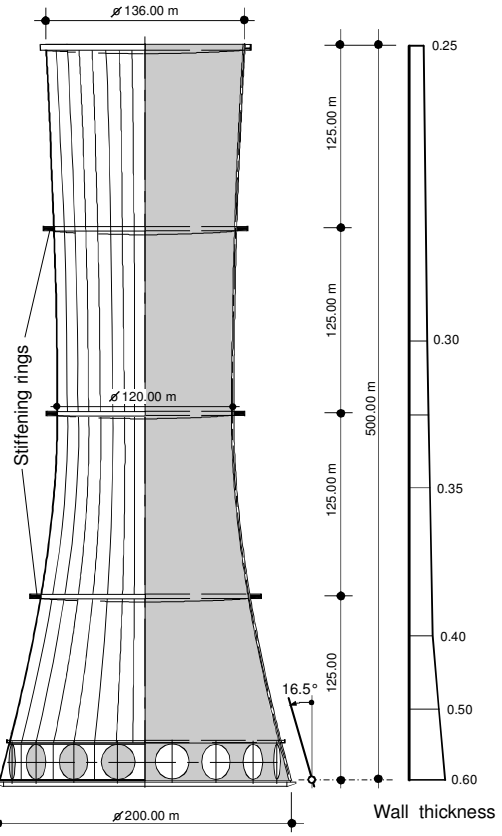

Figure 3: Solar tower of 500 m of height

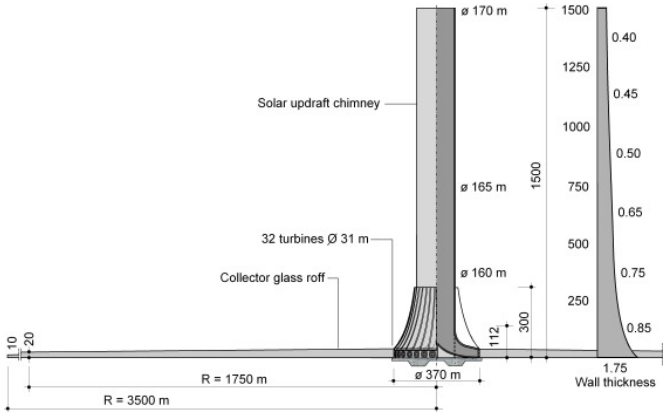

Figure 4: Overview over components of a SCPP

SCPPs are the most sustainable natural resources for electric power generation. They copy the daily solar-thermal air motion in the atmosphere producing electric energy completely free of CO_2-emissions. However, up to date none SCPP has been brought to reality, except for one 50 kW-prototype, erected 1982 in Spain under the guidance of J. Schlaich (Schlaich *et al.* [4]), a pioneer of this technology. This prototype power station worked successfully for more than 6 years. The efficiency of such power generation depends mainly on the size of the collector area and on the height of the chimney, both reasons for the enormous dimensions of SCPPs: Collector diameters up to 7 km and chimney heights up to 1500 m are on pre-design. Figure 5 shows a collection of several possible solar chimneys, all compared to the highest natural draft cooling tower at Niederaussem.

From a load-carrying viewpoint, solar chimneys are extremely enlarged, over-dimensioned NDCT shells, demonstrating all those problems known to cooling tower designers from half a century of experience, namely:

- High compression stresses under deadweight D, wind action W and service temperature T,
- tendency to vertical outside cracking under D, W and T,
- high sensitivity to shell buckling instabilities under D, W and wind suction S,
- forced wind vibrations in the upper chimney part eventually leading to dynamic instabilities,
- strong sensitivity to soil-structure interaction phenomena,
- interestingly a natural safety margin against seismic actions because of low 1st eigenfreqencies,
- stress and thermal fatigue phenomena of the required high-performance concrete,
- durability problems towards the end of a SCPP's service live duration (designed for 80÷120 years).

The structural design of such a solar chimney is an optimization process to compromise between several of these conflicting key points, as the presentation will point out (Backström *et al*. [1]). As example, Figure 6 shows the first three buckling modes for a 1000 m solar chimney with upper edge member and nine intermediate stiffening rings, designed for high performance RC 70/85.

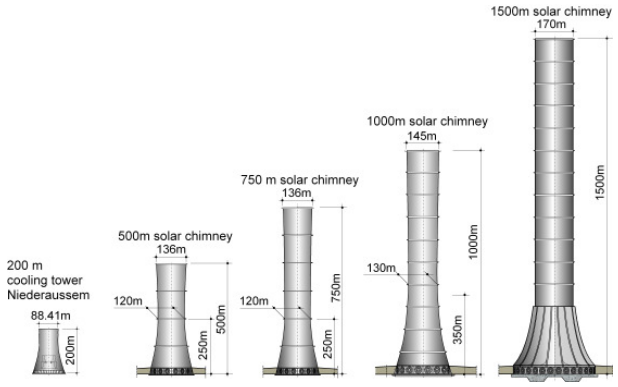

Figure 5: Solar chimneys of different height

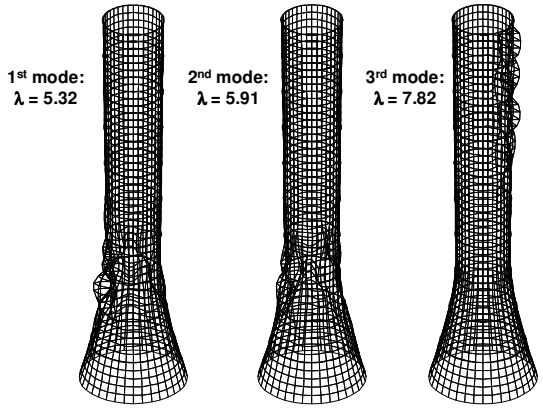

Figure 6: Buckling modes of 1000 m solar chimney

4. Summary

The presentation will illuminate the role of shell structures in power generation technology, in presence. Due to the worldwide rising consciousness for sustainable, CO_2-free energy production, this role is expected to grow enormously in future SCPPs.

Acknowledgement: The second author is deeply indebted to the Volkswagen Foundation, Hanover, for financial support. All authors thank Dipl.-Ing. M. Graffmann, Krätzig & Partner, for valuable contributions.

References

[1] Backström TW von, Harte R, Höffer R, Krätzig WB, Kröger DG, Niemann H-J, Zijl GPAG van. State and Recent Advances of Solar Chimney Power Plant Technology. Submitted to *PowerTech*.

[2] Busch D, Harte R, Krätzig WB, Montag U. New Natural Draft Cooling Tower of 200m of Height. *Engineering Structures* 2002; **24**: 1509-1521.

[3] Krätzig WB, Harte R, Lohaus L, Wittek U. Naturzugkühltürme (Natural draft cooling towers). Chapter X in *Betonkalender* 2007, Vol. 2, 231-322. Ernst & Sohn, Berlin.

[4] Schlaich J, Bergermann R, Schiel W, Weinrebe G. Design of Commercial Solar Updraft Tower Systems, Utilization of Solar Induced Convective Flows for Power Generation. *Journal of Solar Energy Engineering* 2005; **127**: 117-124.

Proceedings of the 6th International Conference on
Computation of Shell and Spatial Structures
IASS-IACM 2008: "Spanning Nano to Mega"
28-31 May 2008, Cornell University, Ithaca, NY, USA
John F. ABEL and J. Robert COOKE (eds.)

Numerical tools in structural optimization

William BAKER, PE, SE, Alessandro BEGHINI, Ph.D.*, Juan CARRION, Ph.D., Aaron MAZEIKA, PE, Arkadiusz MAZUREK, Ph.D.

*Skidmore, Owings & Merrill, LLP
224 S. Michigan Av. Chicago, IL, 60604
alessandro.beghini@som.com

Abstract

Structural optimization attracts increasing interest in the building industry, especially in the design of high-rise buildings. By selectively distributing the material in the structure, the efficiency of the resulting design can be optimized, often resulting in an aesthetically pleasant form.

The paper describes how engineers at Skidmore, Owings and Merrill, LLP are employing several optimization tools for the conceptual development of innovative structural/architectural topologies. These methods include tracing of principal stress trajectories, evolutionary structural optimization and a variety of other techniques based on both gradient methods and genetic algorithms.

1. Introduction

The numerical optimization tools available to engineers are various and their utilization depends on the specific project or application considered. These tools include: principal stress trajectories, evolutionary structural optimization, shape (or form) finding amongst others. Scripting plays a major role in enabling the engineers to access the advanced programming interface (API) of commercial software and to utilize several of their built-in functions within coding of optimization algorithms. Engineers at Skidmore, Owings & Merrill LLP (SOM) have developed a simple algorithm to allow tracing stress trajectories in 2D problems such as in the definition of the lateral wind-resisting system for a high rise building. Commercial software employing gradient based optimization has also been successfully applied at SOM for topology and shape optimization of several potential high-rise projects. Recently, genetic algorithms have been explored to incorporate a new generation of improved scripts allowing wider searches for efficient structural solutions.

2. Principal stress trajectories

Principal stress trajectories represent the natural flow of forces in a structure and are computed according to the following equations, which are derived from Mohr's circle (see Fig. 1 on the left for notation in case of plane stress state):

$$\tan 2\varphi = \frac{2\tan\varphi}{1-\tan^2\varphi} = \frac{2\tau_{xy}}{\sigma_x - \sigma_y} = A(x,y) \tag{1}$$

$$\tan\varphi = \frac{dy}{dx} = -\frac{1}{A} \pm \sqrt{\frac{1}{A^2}+1} \tag{2}$$

The solution of the above equation leads to two sets of characteristic lines (see Fig. 1 on the right).

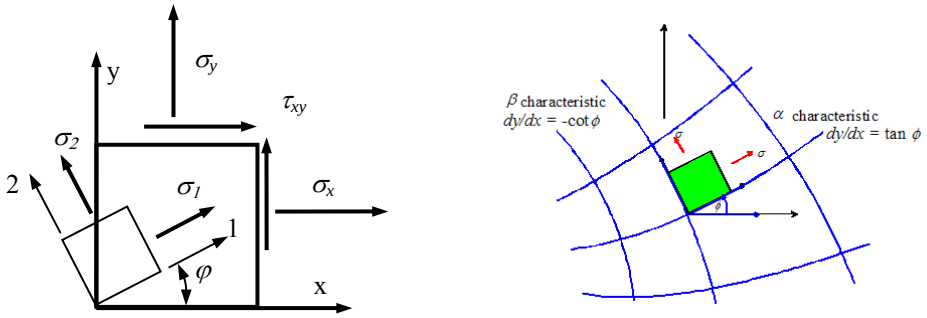

Fig. 1: Nomenclature in principal stress trajectories (left) and characteristic lines (right).

The partial differential equation (1) is solved by finite difference method through a visual basic script in Autocad to define the lateral wind-resisting system in a high rise building.

This approach has been utilized in several competitions for potential projects as shown in Fig. 2. The resulting diagrid systems have both structural and architectural value since they are structurally efficient and esthetically appealing.

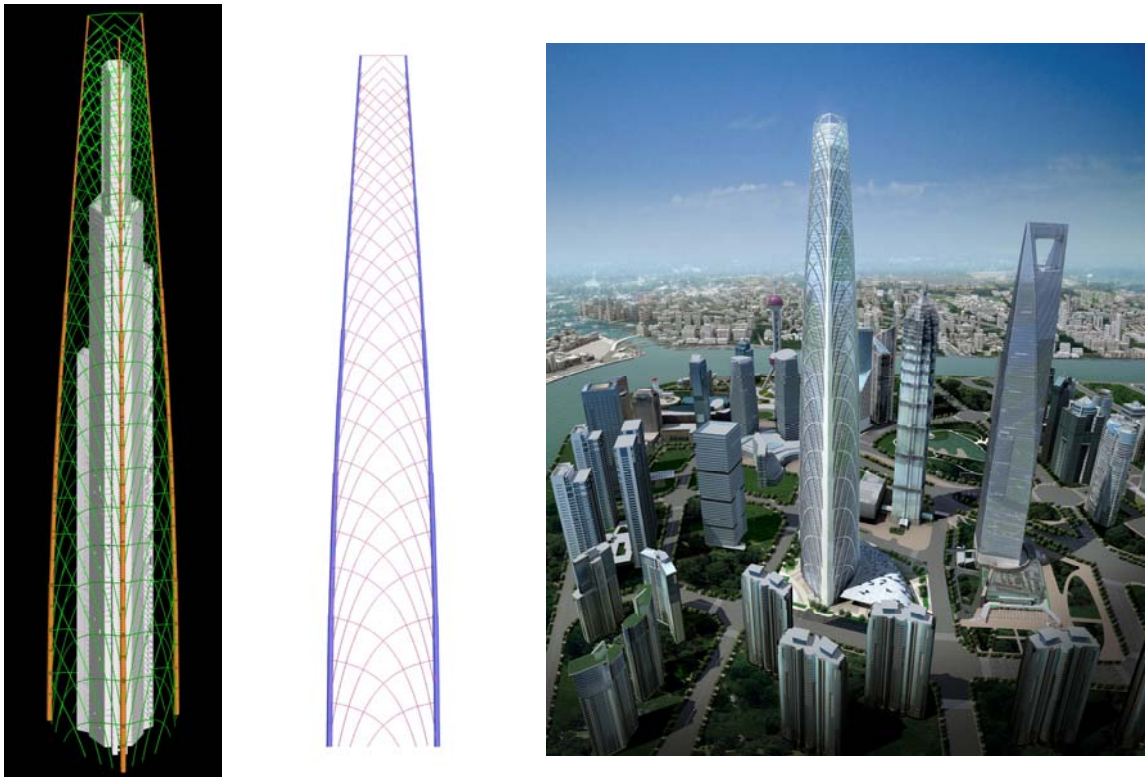

Fig. 2: Definition of the lateral system for a high rise by principal stress trajectories (left) and architectural rendering of the building (right).

3. Gradient Based Methods

Another approach successfully applied in shape finding has been the shape optimization algorithm within the Optistruct module of the commercial software Altair Hypermesh. The approach in this software is gradient based, therefore having the disadvantage of being influenced by the initial conditions. However, for relatively simple problems and starting from a reasonable estimated solution, the resulting shape is often the global optimum rather than the local minimum. This algorithm has been successfully utilized for the design competition winning proposal for a project in Asia (see Fig. 3 for shape evolution during optimization). The building shape has been derived considering the minimization of the building top displacement under lateral pressure and with the constraint of a constant inside volume.

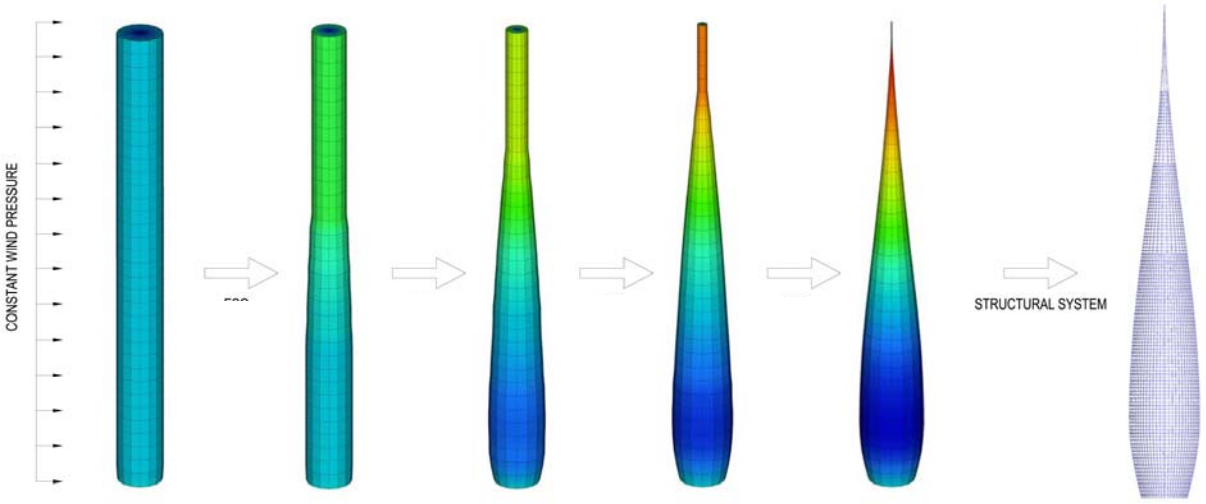

Fig. 3: Evolution of building shape to optimally resist lateral wind pressure.

4. Genetic Algorithm

The dependency of the solution on the initial condition in gradient based algorithms imposes a severe restriction in structural optimization problems. For relatively simple problems, the engineer would typically have an idea of the optimal shape. Therefore, gradient based methods can be used to refine the initial approximation. However, for more complex problems, the shape used for the initial conditions and, therefore, the optimized solution may represent a local optimum, whereas the global optimum is a rather different and unknown shape.

Genetic algorithms are search procedures based on the mechanics of natural selection (Goldberg, 1989). In a genetic algorithm search, an initial population is generated using random values for the design variables. At each generation, a fitness (or objective) function is used to evaluate each member of the population. Based on the results of the fitness function, well performing genomes are maintained, but poor performing ones are eliminated and replaced with an equal number of new ones formed by a variety of basic functions. These include reproduction, where top performing genomes are maintained in the next generation, crossover, where a new genome is formed from a combination of two well performing parent genomes, mutation, where a well performing genome is modified slightly, and the infusion of new blood, with the addition of new random genomes. The search is conducted through successive generations of constantly changing populations with typically improved values of the fitness function at each generation.

Engineers at Skidmore Owings and Merrill have started to explore the application of genetic algorithms to the design of high-rise and complex building structures. The algorithm used at SOM combines an in-house developed genetic algorithm search code (written in Visual Basic .NET) with a commercial finite element software (Strand7). Through the Strand7 API, the genetic algorithm communicates with the finite element solver

and obtains the required response quantity to evaluate the fitness function for the different members of the population at each generation.

The genetic algorithm for structural optimization was verified by solving a shape optimization problem similar to the project in Asia mentioned earlier: minimization of the top displacement of a building with radial symmetry and subjected to lateral pressure. A population of 100 building was used at each generation. Fig. 4 shows the shapes of the top performers at generations 1, 7, 11, 65, 77, and 279. It can be observed that the final shape obtained using the genetic algorithm is similar to the one obtained using the gradient based approach.

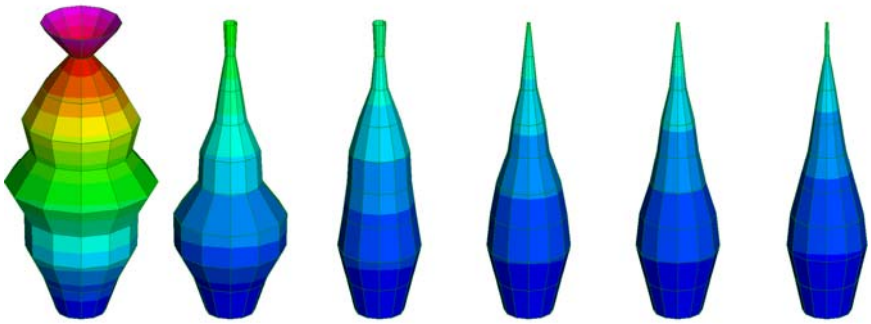

Fig. 4: Evolution of building shape using genetic algorithms.

Conclusions

A variety of numerical optimization tools are available to engineers for design applications. These tools include principal stress trajectory methods, evolutionary structural optimization, shape (or form) finding and genetic algorithms. The specific application of each of these methods depends upon the problem considered and has advantages and disadvantages. Optimization approaches employing a variety of these methods are most likely to result in the optimum solution for a given problem.

References

Goldberg, D. E. (1989). *Genetic Algorithms in Search, Optimization, and Machine Learning*. Addison Wesley Longman, Inc, Indiana, U.S.A.

Proceedings of the 6th International Conference on
Computation of Shell and Spatial Structures
IASS-IACM 2008: "Spanning Nano to Mega"
28-31 May 2008, Cornell University, Ithaca, NY, USA
John F. ABEL and J. Robert COOKE (eds.)

Design process, detailing and examples of non-traditional structures

Christian STUTZKI*, Hiroki TAMAI, Joshua BUCKHOLT

*Professor, College of Architecture, Illinois Institute of Technology
3360 S. State Street, Chicago, IL 60616, USA
chris@stutzkiengineering.com

Abstract

Modern light weight structures like facades and domes, consisting of aluminum, steel, and glass are designed around the architectural design intent, not around well established engineering standards. These design ideas try to "push the limits" in many respects, and create new challenges for the engineering. In fact these attempts to "push the limits" are often times the driving force behind the slow evolution of engineering methods and material applications. During this design and engineering process the building codes play an important guideline in order to prevent unsafe buildings. Most modern building codes allow overriding their simplified rules with more in-depth studies, tests, and numerical simulations. In the beginning of some innovative design processes these studies are pilot studies first, and require very careful judgment when the field of former experience is extended into new areas. .

1. Introduction

This paper is about examples of these design processes for innovative structures. Some observations about typical developments are described, trying to derive "principals" of knowledge evolution in this field of engineering. Several examples are from the field of façade systems and cladding systems are presented

2. The design process

2.1 Building codes and their role

Building codes are defining sets of rules that specify the minimum acceptable level of safety for constructed objects such as buildings and non-building structures. The main purpose of the building codes is to protect public health, safety and general welfare as they relate to the construction and occupancy of buildings and structures. The building code becomes law of a particular jurisdiction when formally enacted by the appropriate authority. Building codes are generally intended to be applied by architects and engineers, but are also used for various purposes by safety inspectors, environmental scientists, real estate developers, contractors and subcontractors, manufacturers of building products and materials, insurance companies, facility managers, tenants, and others.

2.2 Design Professionals and Their Role

Architects and engineers are design professionals—we'll call them "DPs"—in the business of designing dreams. DPs operate in a very sophisticated, technical and complex world of enormous time demands and requests to achieve the impossible, or something just short of impossible (whether due to budget, design, or time constraints). The DP must produce a design that obeys both the laws of man (compliance with building codes, etc.) and the laws of nature (compliance with the laws of gravity, weather forces, etc.), and at the same time it must fulfill the Owner's vision, budget and time requirements. Usually a formidable task, to be sure.

2.3 The Development of the Building Design

the building design and its structural concept is embedded in an iterative process with several loops. This process is also a sequence of decisions, based on criteria made on a group of options or alternatives.

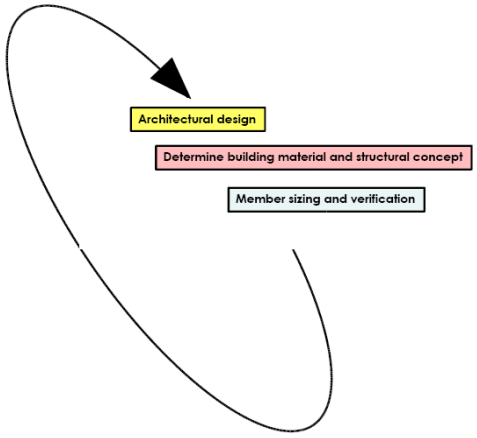

Figure 1: Typical design sequence

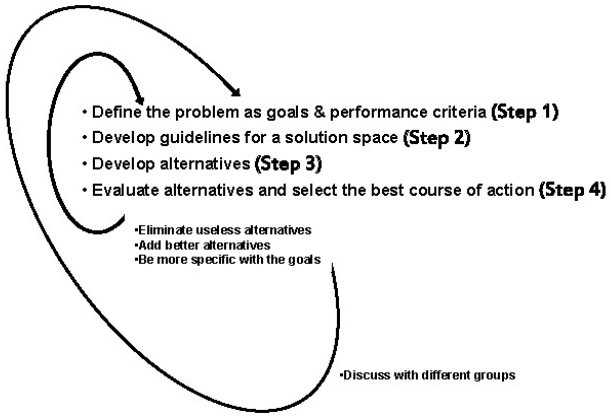

Figure 2: Decision processes during design

Often times these steps are slowed down by confrontation of the engineer, armed with the knowledge of the building codes, rules of the trade, specifications, etc. and the architect, who is caught by surprise by the engineer's views and arguments. Both may lack this necessary understanding of physical concepts and may find themselves in positions of defense, caused by this deficiency. Building codes, Design manuals, material specifications, analysis software, the engineer's whole arsenal, do not offer this knowledge.

2.4 Successful development of a building and it's structure

This is based on this internalized basic knowledge and curiosity about physical concepts. The building codes are used as guidelines (and legal support documents), not as barriers. The computer software is used to understand the design options in simulated models. These steps help to evaluate options and develop challenging, seemingly impossible design options into feasible ones.

2.5 Aspects of the design process of non-traditional buildings

All examples presented in the following part contain one or more of these challenges and they required thinking "back to the basics" of physical principles and logic considerations. They required a lot of verbal communication, supported by hand sketches, followed by enormous "legwork" of numerical studies. In each case the solutions required careful judgment, since there were no precedents available. These steps beyond the rules of design manuals, and beyond codes and specifications typically start with a large amount of numerical simulations and physical tests of specimen. After a while the larger context becomes a bit clear, and simplified models can be developed tested by just a few calculations. This is often good enough to serve as reliable solutions for an actual design process of a structure.

In a later period this whole new approach, if used more frequently in the future, will be picked up by researchers yielding in Ph.D. theses, and, in a later period, may be boiled down to new clauses and equations in design manuals and specifications (see Figure 3)

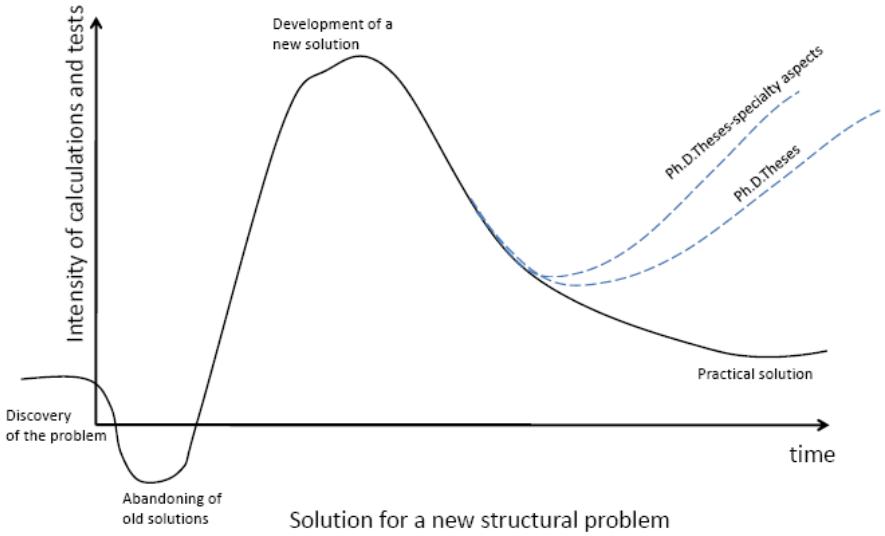

Figure 3: Problem solving diagram for details of non-traditional buildings

3. Examples

3.1 Structural glass canopy with a fail-safe design approach

The canopy consists of triangular narrow glass panels with varying slope, approx. 18 ft. long, each attached with 3 point supports (rotules) to undulating upper and lower steel pipes. The lower steel pipe is propped to the lower support points every 24-6"; the upper steel pipe is mounted to cantilevers from the upper support points also every 24-6". The steel props from the lower support points and the glass panels form a spatial truss structure, triangular in side elevation, with the glass as the upper truss member in tension. This use of the glass as a structural component requires special attention during engineering, manufacturing and installation.

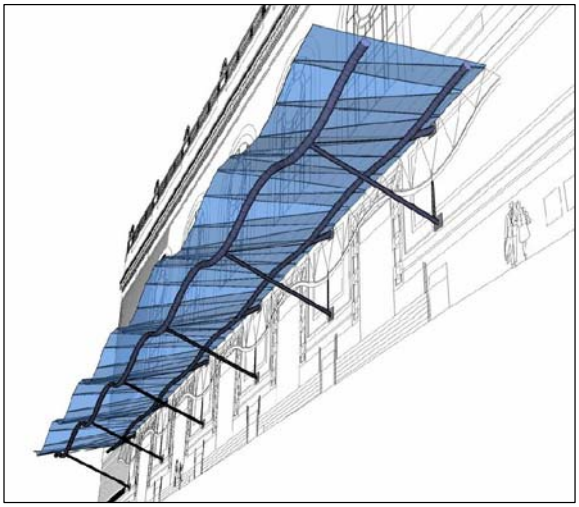

Figure 4: Glass Canopy

3.2 Effects of Prefabrication on Façade Design

To facilitate the façade construction of a mid-rise condominium building, the façade is to be comprised of "Mega Panel" units individually prefabricated and installed. While "Mega Panel" prefabrication in this case allows for a more complex architectural concept to be realized, this architectural freedom also imposes considerable restrictions for each of the panel's structural considerations. The effect of prefabrication and installation processes must be considered throughout all portions of the design to ensure a façade system that

meets performance specifications. Factors with the highest influence on the structural design relate to the high degree of adjustability within panel and anchorage connections that must be achieved and maintained to ensure proper installation and performance of the panels. Consideration is given to concrete and panel deflections under dead, wind, live, and seismic loading, the variability in the concrete and panel construction, lifting points, and field welding restrictions that all must be accommodated by the design before the panels are constructed.

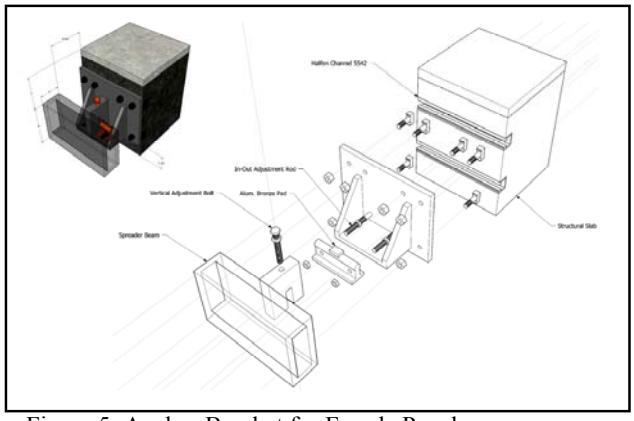

Figure 5: Anchor Bracket for Façade Panel

3.3 A compact, composite, high-strength, fatigue-resisting moment connection for a minimal structure'

A row of trellises for a residence is supported by a minimal steel structure. The steel structure consists of outriggers and a "free-form" hub, manufactured with cast steel; and a vertical post out of bar stock. The 11 ft long outriggers generate high moments at the connection of the casting to the vertical bar stock. This connection was developed to be adjustable during installation, to be fatigue-resistant as to the casting, and to be able to transfer forces as if it was a full penetration weld. The solution was a high-strength post-tensioned insert with a high strength injected cement-resin compound, all within a very small cavity in the casting and in the post.

Figure 6: steel support of a trellis

3.4 Separation of a high glass storefront from building movements in a high-seismic zone

The challenge for this project is a 20 ft. high glass store front of a 641feet tall high rise building. The building is located in a high seismic zone in California, the anticipated building movements at the top of the glass wall, at the second floor level, is almost 4". The monolithic glass wall is supported by glass fins and is supposed not to break during an earthquake. The solution was to isolate it horizontally from the main building, and design a compound system consisting of tempered glass and structural silicone, that stands on the ground on its own. The corner support at the top is a folding-sliding mechanism that facilitates the building movements and the transfer of forces.

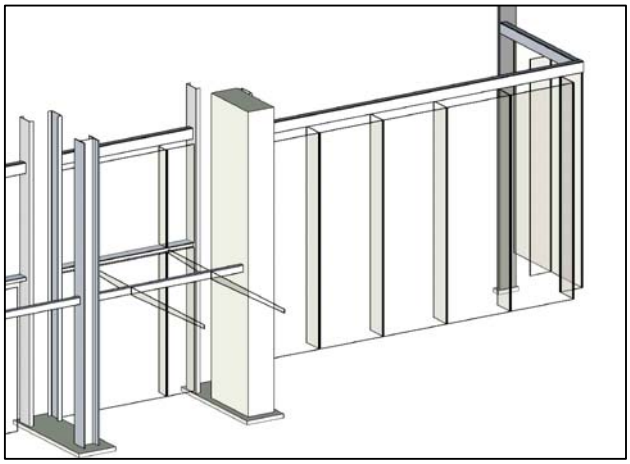

Figure 7: 20 ft high glass fin wall

Proceedings of the 6th International Conference on
Computation of Shell and Spatial Structures
IASS-IACM 2008: "Spanning Nano to Mega"
28-31 May 2008, Cornell University, Ithaca, NY, USA
John F. ABEL and J. Robert COOKE (eds.)

Opportunities and risks with free-form design

Hans SCHOBER, Stefan JUSTIZ, Kai KUERSCHNER

Schlaich Bergermann and Partner LP
555 8th Avenue, Suite 2402
h.schober@sbp.de

Abstract

Three-dimensional computer-aided free-form design, initially developed by the automotive and aerospace industry, has allowed the designer to develop non-regular lines and surfaces, the so-called free forms.

The structural system for these free forms can be shells, membranes or grid shells that can be analyzed and designed with finite element analysis. Using CAM/CNC, there can be a direct transition from the computer model to manufacturing.

As with any new tool, free-form design presents opportunities and risks.

One risk is that this design tool may be used too freely and in an incompetent manner or that irresponsible use may be made of this new tool, with "aesthetics" as the only driving force in the design and with a disregard of structural logic, responsible use of materials, and ease of manufacture and construction.

To create structurally and aesthetically optimized structures, the free-form design of the architect should be used to illustrate the architects' design intent. This then provides an opportunity for the structural engineers to develop a variety of logical and efficient structures. The final goal of this development is to derive efficiency, economy and beauty from the flow of forces in freely curved lines and doubly curved surfaces.

This paper illustrates these risks and opportunities of freeform structures in two constructed examples.

1. Architecturally defined shapes

The free-formed shape for the one-mile long glass canopy of the Milan Trade Fair designed solely by the architect incorporate the neighboring Alps into the overall shape of the sculptural roofs. Like the natural landscape, the geometry is neither repetitive nor described by mathematical algorithms or derived from typical structural form finding.

The distribution of single and double curvature over the canopy surfaces is very inhomogeneous. Large regions of low curvature in which pure bending with tall T-profiles dominate. These regions allow the use of simple four-bar-nodes and plane quadrilateral panes. In the double-curved regions with warped quadrilateral grids, the additional diagonals necessary for covering with plane glass panes help to transform the structure into an efficient shell. In this case the loads are mainly transferred by membrane forces, making optimum use of the material input made possible by exploiting the natural geometric stiffness of double curvature and permitting larger support-free regions.

At the main entrance, the so called 'Logo' soars like a volcano 37 m into the sky thus being easily recognized from afar as the symbol of the new trade fair (fig. 1d). The double curved shape merges on bottom into a flat horizontal roof (fig. 1a and e). thus creating huge bending moments even in the double curved areas of the logo resulting in a structure that was not feasible. The overall form and the support conditions did not fulfill the prerequisites of shell action.

To avoid the very deep bar sections needed to resist large and inhomogeneous bending moments, which could no longer be reasonably combined in the nodes due to large torsional angles of the bars, an 'engineering process' of form finding became necessary to prove the feasibility of the structure.

In this process, which requires some engineering experience, the ratio of bending to shell action was slightly altered in favour of the membrane action by smoothing the regions with peaks of curvature gradients (fig. 1a).. Contrary to classic form finding with only the membrane-type load transfer, this pragmatic approach allowed not only moderately large bending moments in the surface, but also compensated for local extremes.

The Logo-geometry generated by this procedure still corresponded very well with the initial architect's model (fig. 1a) and was finally accepted by the architect. Moreover this revised geometry also helped to reduce many manufacturing problems such as the reduction of torsional angles which have to be resolved by the node detail. Thus, this improvement was also heartily welcomed by the fabricator.

2. Structurally optimized shapes

The skylight over the courtyard of the historical Odeon in Munich (fig. 2) was designed in a close cooperation between architect and engineer in an iterative process until the result satisfied aesthetic, structural and economic requirements.

The architects' design intent for the irregular shape in plan was illustrated by a smooth free-form created with Rhino (fig. 2a).

Since such a freeform shape can only be covered by triangular glass panels, the grid was created by projecting a regular flat triangular grid onto the curved surface.
Geometrical shapes do not usually lead to a proper membrane oriented response. The so called minimal surfaces are identical to a homogeneous membrane stress state that can be obtained for membrane structures by a computer simulation. A similar procedure was developed for this grid shell structure. The permanent loads have been applied to the inverted hanging model (fig. 2b). Cables with a small extensional stiffness have been used for the grid instead of slats. The cables are subjected to prestressing forces as a stress and form controlling load case. A homogeneous prestressing force was applied in the first step and a geometrically nonlinear calculation was applied driving the initial shape. Only the z-component of the nodes were carried over to the next step of the nonlinear analysis.
In subsequent steps, the prestressing force in the cables are varied to achieve an optimum stress state and shape which is also a key parameter for aesthetical appearance (fig. 2c).

Because the Odeon is a listed building, the roof had to be invisible from the outside. Therefore the rise of the roof and thus the curvature are rather small, making the structure even more susceptible to buckling than all optimized structures are. In consequence, an extensive study of the buckling behaviour was necessary and governed the final sizes of the mullions with sections of 50mm x 70mm to 50mm x 90mm.

This example demonstrates, that structurally optimized shapes result in highly transparent and filigree structures which combine efficiency, economy and beauty.

References

[1] Schober, H., Kürschner, K.: Meraviglioso
Civil Engineering, Volume 75, Number 12, December 2005, p. 36-43

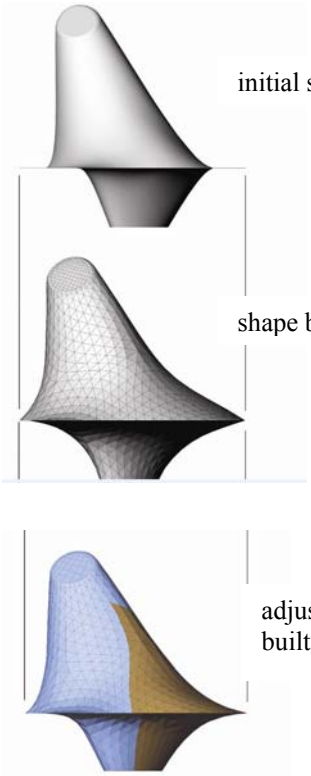

a) Initial shape compared to optimum and adjusted shape

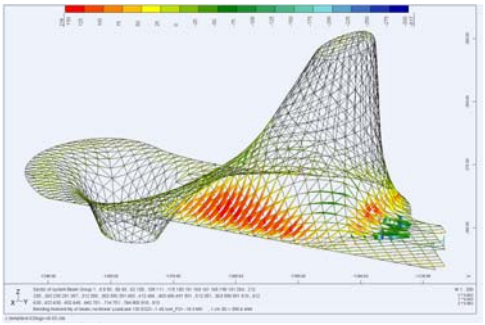

b) Bending moments (red = maximum bending)

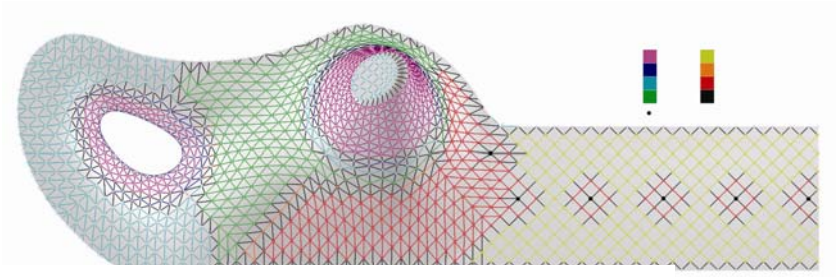

c) Depth of member T-sections (purple = 80mm, red =

d) Photo of Logo structure

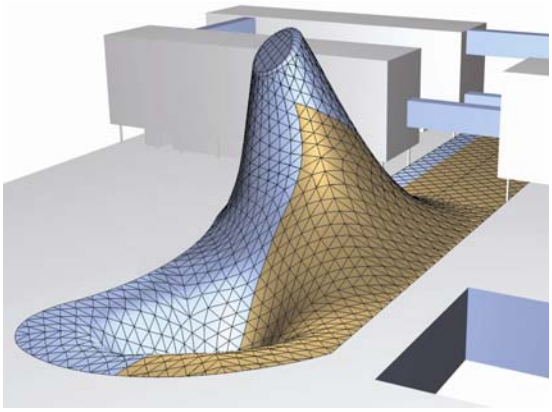

e) Surface model of Logo structure

f) Photo of critical area

Figure 1: Logo structure of new trade fair Milano, Italy.
Architect: Massimiliano Fuksas, Rome, Italy

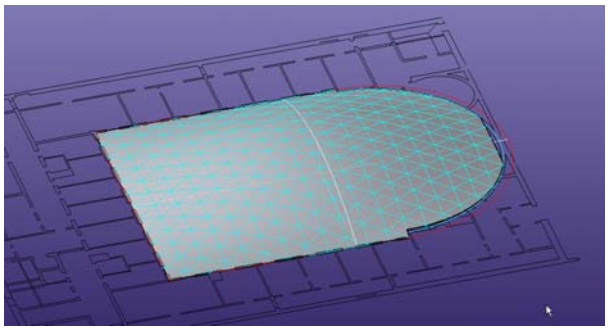

a) Smooth free-form shape

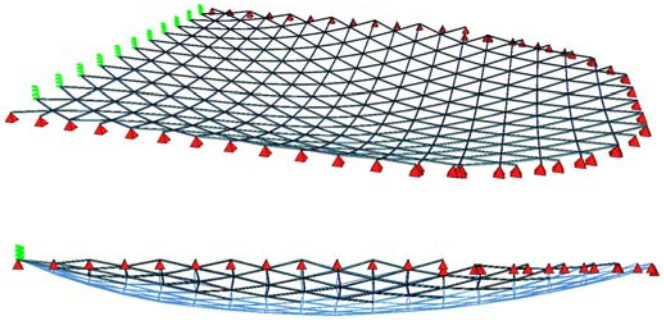

b) Inverted hanging model

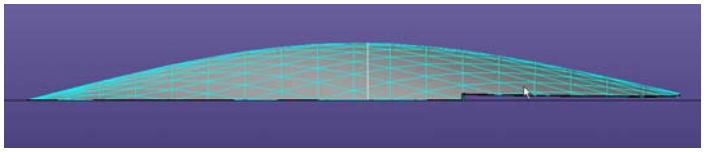

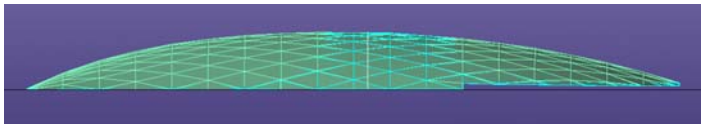

c) Shape before (top) and after (bottom) optimization

d) Photos of courtyard roof

Figure 2: Skylight over courtyard of historic Odeon, Munich, Germany
Architect: Ackermann und Partner, Munich, Germany

Proceedings of the 6th International Conference on
Computation of Shell and Spatial Structures
IASS-IACM 2008: "Spanning Nano to Mega"
28-31 May 2008, Cornell University, Ithaca, NY, USA
John F. ABEL and J. Robert COOKE (eds.)

Novel space frame based on Golden Ratio, 5-fold symmetry, and the fractal HyperFrame system

Chris KLING*, Hiroki TAMAI†, Nicola D'SOUZA°

*President, †VP Structural Systems, °VP Architectural Design
AURODYN, Inc. 3008 Redstone Lane, Boulder, CO 80305
ckling@aurodyn.com
www.aurodyn.com

Abstract

This paper presents a novel space frame system that allows potentially richer design variety for structures while maintaining its unique geometric integrity. The geometry of this space frame system (the angles between struts at joints and the proportion of the member lengths) is based on the Golden Ratio. Also found in nature and often associated with growth patterns, the Golden Ratio exhibits additive and multiplicative properties. These unique properties are taken to great advantage by the AURODYN HyperFrame recursive fractal patented truss system. The principles of this space frame system and example structures are presented in this paper.

1. Introduction

Space frame structures have been widely applied in many construction industries since the 1950s, in order to cover long-span areas or to constitute components of mega-structures. Today, their structural and constructional efficiency as well as adaptability to architectural geometry are well acknowledged by engineers and architects. However, when a traditional space frame system is applied to derive a complex shape for a roof or a building, the advantages in manufacturing are lost to a maximum inventory situation caused by forcing the cubic lattice to adhere to a free-flowing form. Furthermore the topology of the mesh space frame has a definite impact on the aesthetic appeal of the final structure and often constitutes an "impedance mismatch" between a cubic lattice mesh and organic geometry. This system follows Steve Baer's pioneering and remarkable discoveries in Golden Ratio based space frame design conducted in the sixties and seventies. Surprisingly this geometry has not been studied or utilized significantly and its structural benefits remain unexplored to this day.

2. Review of Golden Ratio and Golden Geometry

Golden Geometry is defined as geometry based on the Golden Ratio. Many natural systems exhibit all or some subset of Golden Geometry, as do many structures and mathematical systems extensively studied for centuries. For example, the well-known Platonic solids – tetrahedron, cube, octahedron, dodecahedron, icosahedron – exhibit either the entire or subsets of the symmetries found in Golden Geometry, as do the relatively recently discovered class of crystal structures known as quasi-crystals.

2.1 The Golden Ratio

The Golden Ratio, also known as Phi (Φ) is a mathematical relationship of quantities in which the relationship of the smaller quantity to the larger quantity is the same as the relationship of the larger quantity to the sum of the two quantities. The name derives from the fact that this ratio has been long considered aesthetically ideal, or "Golden," and is found in art, sculpture and architecture throughout history. More recently, discoveries in the field of phyllotaxis and biology have shown that this number is also involved with growth patterns in the living world.

The Golden Ratio is an incommensurable irrational number. Mathematically this ratio (larger quantity over smaller quantity) is expressed by the equation $\Phi = (1 \pm \sqrt{5})/2$ and its value is 1.618033981749894… The negative root of this quadratic equation is -0.618033981749894... and its absolute value corresponds to the length ratio taken in reverse order (shorter segment length over longer segment length), and is sometimes referred to as the "Golden Ratio conjugate". It is denoted here by the lower case phi (φ). A series of lengths in the Golden Ratio possess some very unique mathematical relationships.

2.2 Unique Mathematical Properties

Since the Golden Ratio maintains the relationship between the parts and the whole, the ratio has both multiplicative and additive properties [1]. Figure 1 and equation (1) below demonstrate the additive and multiplicative relationships of the series and the equations (2) to (10) list other relationships between the terms in the series:

$$\Phi^2 = \Phi + 1 \tag{1}$$

$1 = \Phi^0$
$\Phi = \Phi^1$
$\Phi + 1 = \Phi^2$
$2\,\Phi + 1 = \Phi^3$
$3\,\Phi + 2 = \Phi^4$
$5\,\Phi + 3 = \Phi^5$

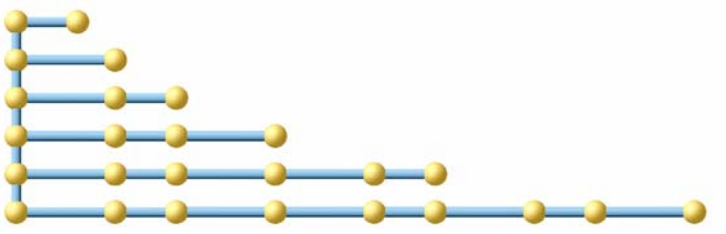

Figure 1: Higher powers of the Golden Ratio may be expressed as the linear combination of two base lengths

Some other interesting relationships between terms in the Golden ratio series:

$\Phi \times \varphi = 1$	(2)	$\Phi = 1 + \varphi$	(5)	$\varphi = 1 / \Phi$	(8)
$\Phi - \varphi = 1$	(3)	$\varphi = \Phi - 1$	(6)	$(-\varphi)^2 = -\varphi + 1$	(9)
$\Phi + \varphi = \sqrt{5}$	(4)	$\Phi = 1 / \varphi$	(7)	$(\varphi)^2 = 1 - \varphi$	(10)

This ratio is also intimately linked to the number 5 and five-fold symmetry as it appears in the pentagram in the relationship between its sides and the diagonals, as well as in the Cartesian coordinates of the vertices and inscribed rectangles of the icosahedron and dodecahedron.

2.3 Icosahedral symmetry and 5-fold symmetry

Icosahedral symmetry represents one of three main ways to partition 3D space regularly from a center point, the other ones being cubic and tetrahedral symmetry. It consists of 3 main sets of symmetry planes: fifteen 2-fold, ten 3-fold and six 5-fold. In addition to having the most number of axes of symmetry, icosahedral symmetry is the only one to have 5-fold symmetry.

In 1986, the world of crystallography, physics and chemistry was shaken in its foundation by the discovery of a new class of molecules: the quasicrystals. These crystals exhibited the forbidden 5-fold symmetry, aperiodicity, and many unexpected qualities.

From a symbolic point of view, the number 5 has often been associated with life and mankind (e.g. 5 senses, 5 fingers) and has given us the quint-essence or 5th essence after the 4 elements of matter (earth, water, air, and fire).

2.4 Golden Geometry system.

The Golden Geometry framework offers icosahedral symmetry at every node and the lengths of the vectors are proportional to the powers of the Golden Ratio. A system based on this geometry inherently possesses all advantages of the unique 3 dimensional mathematical relationships of this vector star [2]. Physical models may be prototyped with the excellent Zometool plastic parts kits (www.zometool.com).

In 1946, Swiss architect le Corbusier published the “Modulor” a scale of proportions based on the powers of the Golden Ratio. The authors do not view the Modulor as a complete Golden Geometry system as it is lacking icosahedral symmetry and exhibits only vectors parallel to the three orthogonal axes X, Y and Z.

The AURODYN HyperFrame recursive fractal truss system is an effort to develop upon the system pioneered by Steve Baer and integrate this geometry into mainstream architectural design and structural engineering.

3. HyperFrame: A space frame system with Golden Geometry and modeling software

3.1 Benefits of Golden Geometry in architecture

Once one has accepted to play by the new rules of Golden Geometry, many remarkable properties reveal themselves. Here is a shortlist of fundamental benefits that become available when the system is applied to ball joint space frame structures for architecture. In this process the geometry vectors become struts and the points become nodes.

3.1.1 Three-dimensional stability with efficient triangulation

The stiffness (and strength) of a ball-joint space frame structure depends mainly on its degree of triangulation. The simplest unit that is spatially triangulated is the tetrahedron. The authors have found that with these golden lengths they were able to generate many different tetrahedra that can be used to create trusses and trussed planes to stiffen node-and-strut structures

3.1.2 Superior connectivity and packing

Because various tetrahedra can be chosen to interface to other tetrahedra through face sharing, these tetrahedral space frame unit cells can be assembled to construct stiff modular structures [3]. Other shapes such as square, rectangles, rhombs, pentagons, hexagons, decagons are also readily available to build 3D polyhedral cells such as regular and irregular boxes, pyramids, prisms, antiprisms, octahedra, tetrahedra, most Archimedean solids, and many others.

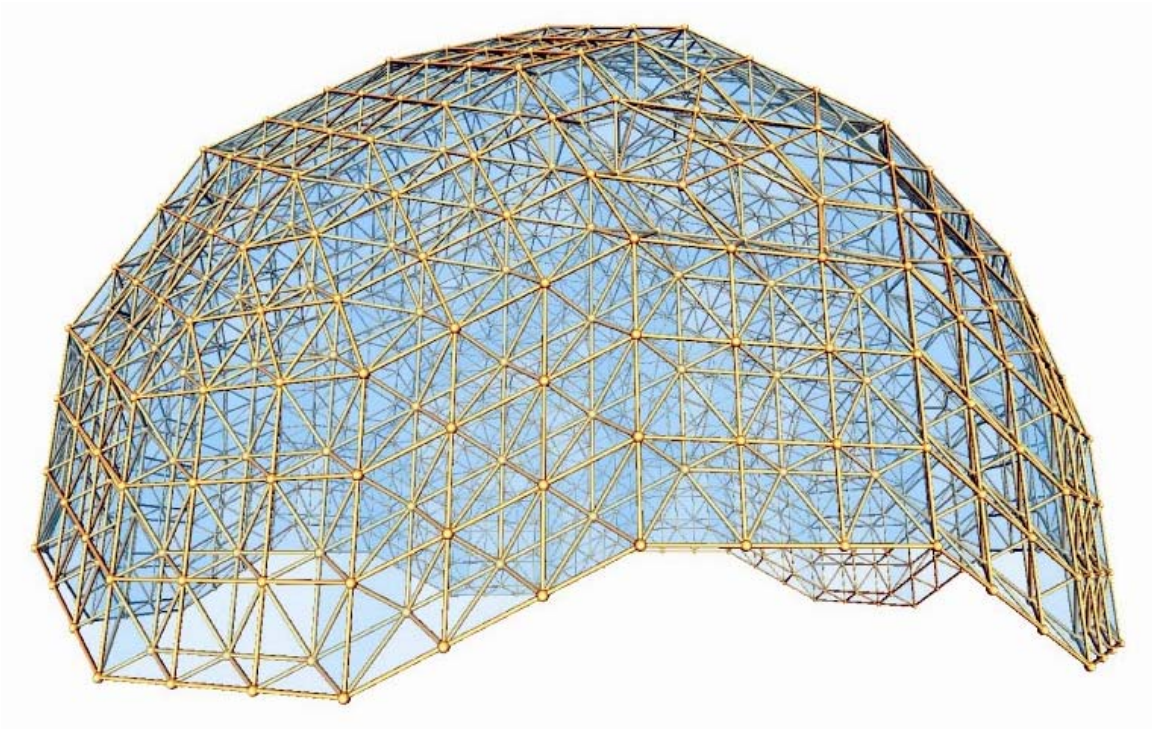

Figure 2: Any Golden Geometry skin model may be stiffened through a network of octet planes

3.1.3 Minimum inventory with maximum diversity

The many tetrahedra that can be built with Golden Geometry have an inventory of only a few dozens different triangular panels. Similarly the edges of these tetrahedra can be built from an inventory of only a dozen and a half different strut lengths.

This minimum inventory leads to economies of scale through mass production, supply chain management and assembly while allowing maximum diversity in the structural shapes and designs. See [4] for an introduction of the seminal concept by Peter Pearce.

3.2 Recursive fractal truss system

Equation (1) demonstrates that any power of the Golden Ratio may be expressed as a linear combination of only two lengths. Following this principle the authors set out and discovered that any base vector could be expanded into a series of trusses built with very few parts. This patented system is fractal in nature as the same expansion may be applied recursively unto itself producing a "truss of trusses" or "truss of trusses of trusses" while totally respecting and preserving the Golden Geometry with its precise angles, topology and powers of the Golden Ratio based lengths.

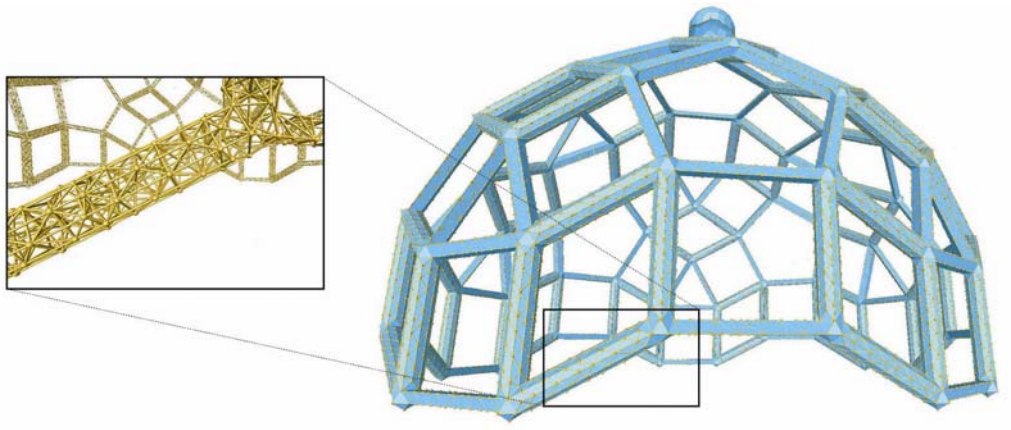

Figure 3: Any Golden Geometry structure may be expanded through HyperStruts trusses and HyperNodes.

3.3 Golden Geometry software

The authors have developed "HyperFrame", a soon-to-be-released CAD software for Golden Geometry. The algorithm and interface of the software are well suited for the unique and unconventional modeling process. It enables users to easily become familiar with the surprisingly diverse yet sophisticated composition of Golden Ratio geometry. In addition, the software has a structural analysis module that graphically shows basic analysis results anytime during the modeling process, so that designers can check the structural behavior of their space frame design. All the models in this presentation were created in "HyperFrame".

4. Conclusion: richness in design variety with scalability at mass production costs

Using this relatively limited kit of parts a large variety of forms can be designed. The geometry easily lends itself to creating space frames for planar, spherical, cylindrical, parabolic, hyperbolic paraboloids and other organically curved roof forms. For all these forms, the basic components types are few and lend themselves for mass-production. These forms can be scaled to create frames for various applications ranging from furniture and houses to bridges, towers and stadiums.

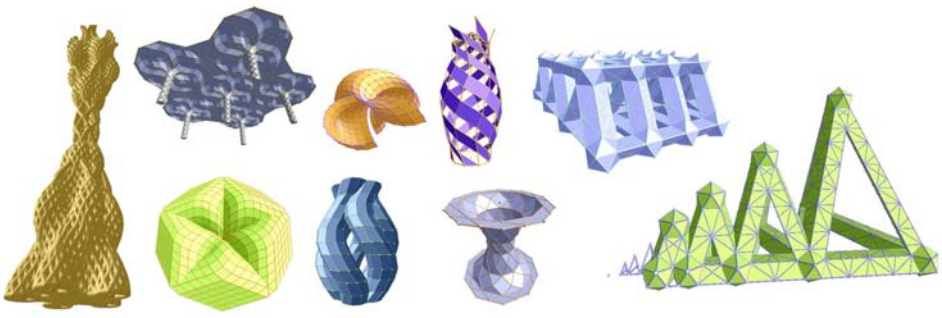

References

[1] Ghyka M. The Geometry of Art and Life (1st paperback edition). Dover Publ. Inc. New-York, 1977; 7-12

[2] Baer SP. Zome Primer (2nd printing). Zomeworks Corporation Albuquerque NM, 1970

[3] Buckminster RB. Synergetics (1st paperback edition). Macmillan Publ. Company, 1982; 135-142, 365-368

[4] Pearce P. Structure in Nature Is a Strategy for Design, MIT Press, 1990; 200-206

Proceedings of the 6th International Conference on
Computation of Shell and Spatial Structures
IASS-IACM 2008: "Spanning Nano to Mega"
28-31 May 2008, Cornell University, Ithaca, NY, USA
John F. ABEL and J. Robert COOKE (eds.)

Determination of warping deformation limits for insulating glass units in cable net facades

Hiroki TAMAI*, PhD, Christian STUTZKI, PhD, Joshua BUCKHOLT, Mathew WEGLARZ

*Stutzki Engineering, Inc.
338 North-Milwaukee-Street
Milwaukee, Wisconsin 53202, USA
hirokitamai@yahoo.com

Abstract

Cable nets façades, in which glass panels are usually supported by so-called patch fittings instead of mullions, are usually designed to allow relatively large overall deflections of cables under wind load. This may cause excessive warping of glass panels close to the corners of the rigid boundary for the glass wall. When insulating glass units (IGU) are used for a cable net façade, their deformations need to be controlled more carefully than a case of utilizing monolithic panels, in order to prevent damage of the sealing material. This paper, first, presents a mathematical model to estimate limit values for the warping of IGUs. Second, the proposed formula to calculate the warping limit is evaluated by comparing to finite element analysis results with a square unit. Third, design of a cable net façade that applied this criterion is introduced. This paper is concluded with evaluation of this design procedure and limit of the formula.

1. Introduction

Cable net façades are a very transparent glazed curtain wall system, in which glass panels are usually supported by prestressed cables via so-called patch fittings instead of conventional mullions. The glass panels are clamped at the corners patch fittings, which, in turn, attached to prestressed cable net. Prestress cables are used in order to reduce the structural member sizes while maintaining structural instability. Because of this transparency, cable net glass façades are becoming more and more popular in contemporary architectural design. On the other hand, the cable nets façades are usually designed to allow relatively large overall deflections under wind load, so that prestress level applied in cables, which control the stiffness of the system, should be in an efficient range. This may cause excessive warping of glass panels close to the corners of the rigid boundary of façades. Therefore, in design, it is important for engineers to properly control the deformations of the each glass panel, while allowing a relatively large overall deformation to the cable net.

Although monolithic glass panels have been used in glass façades of this kind almost exclusively, it is expected that insulating glass units will be increasingly demanded to use when such transparent systems are incorporated with more various building types. The two glass façades for podium and observatory deck of Lotte Super Tower (architectural and structural design by Skidmore, Owings & Merrill LLP) are examples of such cases.

A major difference between design of monolithic glass and that of IGUs is due to the composite characteristics of IGU. The industry standards for IGU are limiting the edge deflection of an IGU to 1/175of the edge length [1]. This is based on tests of typical IGUs in terms of edge deformation and long term performance of the IGU. The long term performance depends mostly on the stability of the primary seal of the IGU. This primary seal consists of an airtight strip of butyl connecting the spacer bar to the glass panels. Tests indicate that the adhesion of the butyl to the glass and to the aluminum cannot be guaranteed, when the edge deflects more than L/175, where L is the length of the edge. This means that when IGUs are used for a cable net façade, their deformations need to be controlled more carefully than a case of utilizing monolithic panels, in order to prevent damage of the sealing material. However, there is not any established design guideline particularly prepared for cable net façade systems supporting IGUs.

In consulting the design of cable net IGU facades of the abovementioned project, the authors developed a method to calculate warping deformation criteria, which should be considered in addition to global cable net deflection, stress and deformation of glass panels due to local bending etc.

2. Methodology

2.1 Mathematical Model

In order to determine the allowable magnitude of warping without testing, a theoretical method is developed to estimate this limit. This method is based on allowable deflections of insulating glass units framed with conventional mullion systems, which is typically L/175. We assume that this value of deflection is small enough to keep the butyl seal undamaged. The method is a simple analogy between max shear deformation along an edge of a bent panel and that of a warped panel.

First, by equalizing the bending deflection limit of typical IGU, L/175, to deflection of simply supported one-way panel expressed by L, corresponding slope angle, γ_{slip}, can be expressed as below.

$$\gamma_{slip} = \frac{L}{175} * \frac{16}{5} * \frac{1}{L} = 0.018 \tag{1}$$

Because the module of elasticity of butyl is considerably smaller than glass and aluminum, its shear deformation along a strip determines the shear deformation of an IGU. In addition, because a butyl strip is negligibly thinner than spacers and panels, a critical slide distance between a glass panel and a spacer, Δ_{slip}, due to a shear deformation at the edge of the panel can be expressed by γ_{slip} as,

$$\Delta_{slip} = \gamma_{slip} \frac{(t_a + t_g)}{2}; \quad t_g = \max\{t_1, t_2\} \tag{2}$$

where t_a, t_1 and t_2 are respectively thickness of air space, glass lite 1 and lite 2. t_g is the larger of t_1 and t_2. This Δ_{slip} is actually the shear deformation responsible for seal breakage.

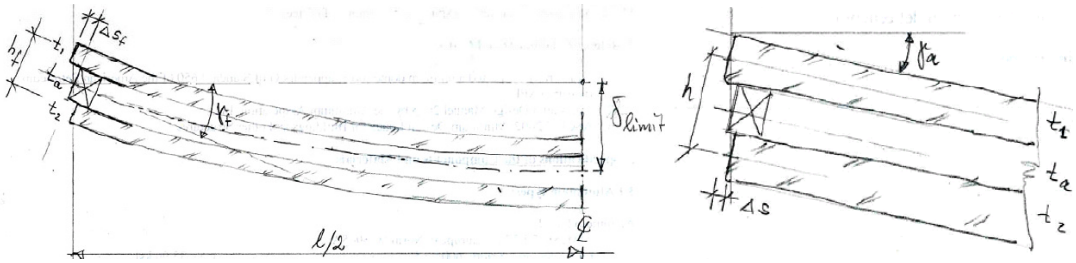

Figure 1: Compatibility of shear deformation and slope angle

Because the limit deflection criteria, L/175, should be valid for the most common glass thickness and air space, i.e. t_g = 1/4" and t_a = 1/2", the sliding limit for the shear deformation Δ_{slip} yields in:

$$\Delta_{slip} = 0.018 * 0.75/2 = 0.007 \text{ in.} = 0.18 \text{ mm} \tag{3}$$

Thus, the limit of slide distance due to shear deformation is defined by the limit deflection.

Next, warping of a rectangular IGU can be evaluated with displacements of its four corner points by eliminating rigid transversal and rotational displacements. It must be noted that, in this approach, bending deformation of glass plates to resist warping is not considered. In most cases, the in-plane displacements are not important for warping evaluation. Therefore, the total warping, W, evaluated as out-of-plane displacement of one corner point in relation to a plane defined by the other three corner points can be calculated by using out-of-plane displacements, V_n (n= 1~4), as

$$W = V_1 - V_2 + V_3 - V_4 . \tag{4}$$

When symmetric warping deformation can be assumed, the out-of-plane displacement in relation to centroid of the panel, V_w, is calculated as

$$V_W = \frac{W}{4}. \tag{5}$$

Therefore, the critical shear deformation between layers of an IGU, γ_{warp}, is estimated by using shorter dimension, say a here, as

$$\gamma_{warp} = \frac{2 * V_W}{a} = \frac{W}{2a} \tag{6}$$

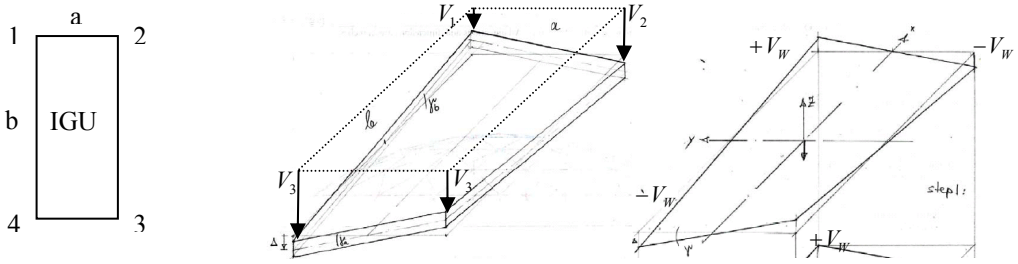

Figure 2: Calculation of total warping

Using equations (2) and (3) with t_a, t_g and γ_{slip} as variables, and equalizing γ_{slip} and γ_{warp}, allowable wapring, W_{allow}, can be calculated as followng.

$$W_{allow} = 0.028\frac{a}{(t_a + t_g)}(inch) \quad or \quad 0.71\frac{a}{(t_a + t_g)}(mm); \quad t_g = \max\{t_1, t_2\} \tag{7}$$

2.2 Validation with a Simple Finite Element Model

Liner finite element analysis with a simple square model indicates that the shear deformation of butyl strips can be predicted by the proposed formula within a practical tolerance range. The tolerance range is estimated to be about +-30%. But, the tolerance highly depends on panels shapes. The range of tolerance will be discussed in more details in the presentation or a full paper including a description of the finite element analysis model.

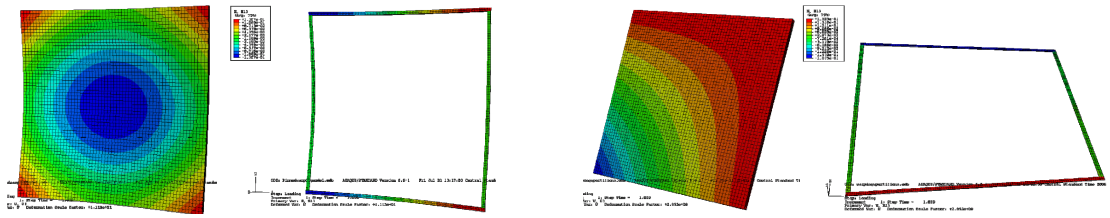

Figure 3: Simple FEA model for evaluation of the mathematical model

3. Examples of Practical Application

This section illustrates the design flow that the authors took for engineering of cable net façades supporting insulating glass units. They are designed for Lotte Super Tower. Their maximum vertical span is about 45 meter. In this project, glass unit sizes are so large that the each glass unit needed to be supported by a mullion frame to reduce individual panel deflection and bending stress. The mullions are hanged on prestressed cable nets via clamping metal works.

The allowable warping calculated by the equation (7) was used as a guideline to determine cable sizes and prestress level, and control maximum cable net deflection. Total warping, W, of each IGU was first calculated by geometric nonlinear analysis of the cable nets and evaluated by nodal displacement of the clamping points. When design became more detailed, accuracy of the analysis was increased by including intermediate structural elements that connect IGUs to the cable net. A few cases close to the estimated warping limit were investigated individually by resorting to finite element analysis. Finite element model needed to be detailed enough, by employing fine-meshed solid elements, to simulate such a complicated structural behavior constituted with rigid material, such as glass, and soft material, such as butyl, and rigid but flexible member, such as aluminum spacer.

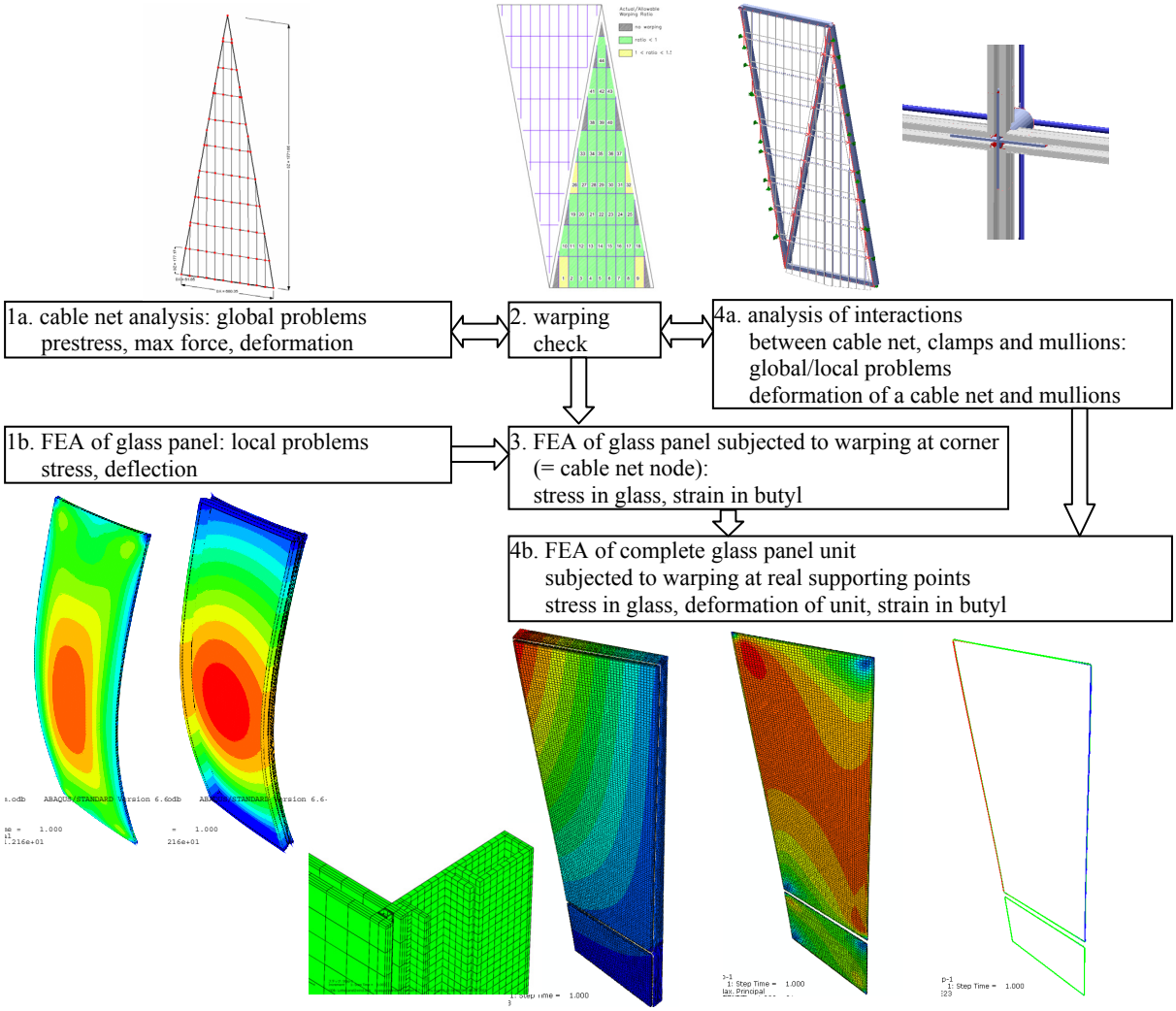

Figure 4: Design flow chart

4. Conclusion and Remarks

The limits of warping deformation of insulating glass units that will maintain sealing adhesion can be estimated by the analogy to shear deformation due to bending. The estimated criteria may be used for preliminary engineering or guideline to determine the overall deformation of a cable net façade incorporated with IGUs. However, the FEA with detailed model or physical tests are suggested to confirm the performances of IGUs. Analyses on rectangular IGUs show the shear strain in longitudinal direction is greater than one along the shorter strip unlike the assumption made in the proposed mathematical model. This may be resulted from bending deformation of mullions accompanied with warping. Further investigation is needed. Similarly, more close attention will be required for application of this mathematical model to irregular shapes.

Acknowledgement

The authors are grateful to Skidmore, Owings & Merrill LLP that we could work on this project as a consultant team and for critical discussion through the project from conceptual study to design development. We also thank them for granting permission for publishing. The first author personally likes to acknowledge Stutzki for fundamental establishment of the mathematical model presented in this paper.

References

[1] Glass Association of North America. GANA Glazing Manual (2004 edn). 2004.

Proceedings of the 6th International Conference on
Computation of Shell and Spatial Structures
IASS-IACM 2008: "Spanning Nano to Mega"
28-31 May 2008, Cornell University, Ithaca, NY, USA
John F. ABEL and J. Robert COOKE (eds.)

Optimal design of unitized structures with curvilinear stiffeners

Rakesh K. KAPANIA*, Pankaj JOSHI, Manav BHATIA, Thi DANG

*Norris and Laura Mitchell Professor of Aerospace Engineering,
Department of Aerospace and Ocean Engineering
Virginia Polytechnic Institute and State University
215 Randolph Hall
rkapania@vt.edu

Abstract

The Multidisciplinary Analysis and Design Center for Advanced Vehicles (MADCAV) at Virginia Tech has been involved in the development of a computational design environment that is capable of designing curved stiffened panels using curvilinear stiffeners. The past work and the current development work of the research group in this area are summarized.

1. Introduction

Ongoing revolution in information management, materials science, computational science and manufacturing technology has made it now possible to fabricate new generation of, mostly custom-built, structures that will have a low part count, built-in multi-functionality, and an ability to tailor the structure according to the design requirements. Termed unitized structures, these structures are formed by adding or building up material as opposed to *Subtractive* (i.e. taking the material away as in machining) or *Formative* (casting) methods of manufacturing. For nearly three years, under a grant from NASA Langley Research Center, and more recently under a NASA National Research Announcement in collaboration with Lockheed Martin, we have been developing a computer environment that will help NASA and US aerospace industry optimally design unitized structures built using such approaches as the Electronic Beam Free Form Fabrication, EBF_3, and will make use of the design flexibility (efficient use of geometry) made possible by these new manufacturing technologies. The environment, *EBF3PanelOpt*, involves an integration of continuous mesh generation, optimization, NURBS to represent curvilinear stiffeners, and commercial finite element software. Here we briefly describe the challenges faced and the methodology developed to overcome them.

2. Optimal Stiffener Placement

The placement of curvilinear stiffeners is defined by the end points of the stiffeners on the boundary of the panel, and the stiffener curve joining these points. A loaded panel geometry is shown in Fig. 1 as an example, and the stiffener curve (modeled as NURBS) design parameterization is shown in Fig 2. A stiffened panel optimization problem aims to find the optimal values for each one of these parameters, and the cross-section values of the panel and the stiffeners. Due to the complexity of the problem, finite element analysis is used to perform structural analysis and a numerical optimization algorithm is used to find the optimal design. The design objective is to minimize the structural weight, subject to buckling and stress constraints.

The design space defined by these parameters is highly nonlinear with the presence of multiple local minima. Hence, when using gradient-based optimization algorithms, it is very important to have a starting point that is close to the global optima. Previous work on unitized structures by Kapania *et al.* [1] dealt with straight and curvilinear stiffeners with end points located a-priori, for which only a sizing optimization was performed.

2. CCMSO/CCRSA

Mulani *et al.* [2] developed an approach for optimal placement of stiffener end points, where only straight stiffeners were considered. A response surface of optimum stiffened panel weight was constructed for different end point locations and optimization using this response surface gave the optimal end point locations. For two

straight stiffeners, the construction of response surface (RS) required 190 simulations using CCMSO/CCRSA approach. Although this algorithm guaranteed global optimization, it was computationally very expensive even for a small subset of design parameters.

3. Meta-modeling approach

This section presents the design methodology using a surrogate model, which incorporates the shape design parameter α and y co-ordinates of the stiffener end points. Involvement of the shape design parameter α makes the surrogate model development methodology complex and it becomes very hard to choose sample points to get a robust surrogate model. To cope with this problem an approach similar to Queipo *et al*. [3] is followed. In this approach first, all the design space is explored for different shape design parameter α. For each value of α all the possible configurations are searched and a configuration, which gives the optimum weight of the panel with curvilinear stiffener, is selected. This design exploration method gives the knowledge that there is a range of α for which a particular configuration of the curvilinear stiffeners gives optimum design. To make this process faster, first a coarse mesh for finite element simulation is used. Once, we have the idea of the design space that contains the optimum design, refined mesh is used in FEM simulation to get the required simulation run cases to obtain a robust meta-model. If necessary, an iterative refinement is used to enforce robustness and validity of the surrogate model.

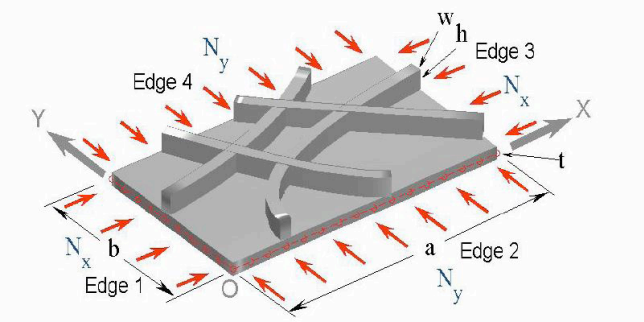

Figure 1: Bi-normal load: Nx = 250kN/m, Ny = 50kN/m, uniform vertical pressure: p = 10000N/m2, fixed: edges1 and 4, simply supported: edges 2 and 3, all aluminum a = b = 2.54m, with displacement constraint = ±0.1m.Initial size and bounds: t0 = w0 = 0.005m; h0 = 5w0; tb=wb=[0.0001, 0.1] m; hb = [0.0001, 0.5] m

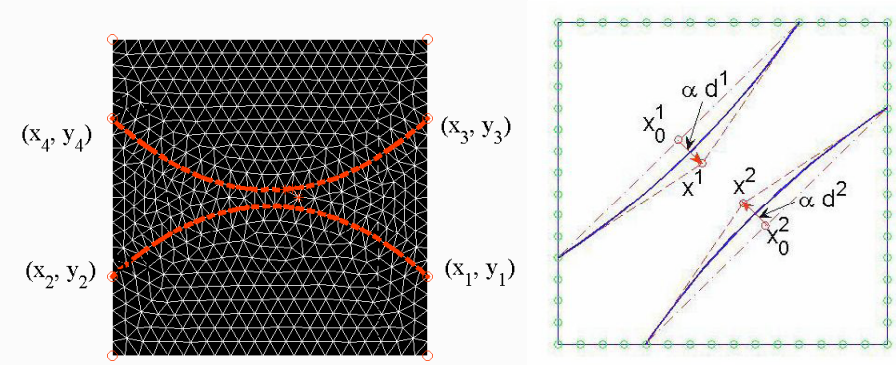

Figure 2: End point co-ordinates of curvilinear stiffeners on *EBF3* panel (left), and shape design parameter α controlling the motion of the two mid points X^1 and X^2

4. Stiffener Effectiveness Approach

A new method, called the *Stiffener Effectiveness Approach*, is developed. A *Stiffener Effectiveness* metric is proposed along with an optimization procedure that can be used to optimize the stiffener locations.

Assuming that all stiffeners are made from a homogenous material, for a given stiffener configuration on the panel, the metric is defined as a function:

$$M(\xi_i) = \sum_{i=1}^{N} \int_0^L I(\xi_i) f_i(w,\xi_i) d\xi_i \tag{1}$$

where, ξ_i, is the coordinate along the i[th] stiffener and is a function of the panel *x*- and *y*- coordinates, *i.e.*

$$\xi_i = \xi_i(x,y) \tag{2}$$

$I(\xi_i)$ is the cross-sectional moment of inertia of the stiffener, and $f_i(w,\xi_i)$ is a function of the displacement $w(\xi_i)$ along the length of the stiffener. This displacement field is obtained from the first buckling model of the loaded unstiffened panel. The choice of this function can be the norm of the displacement, or the gradient or curvature of the displacement along the stiffener length, *i.e.*

$$\begin{aligned} f_i(w,\xi_i) &= |w(\xi_i)|, \text{ or} \\ f_i(w,\xi_i) &= |\nabla w(\xi_i)|, \text{ or} \\ f_i(w,\xi_i) &= |\nabla^2 w(\xi_i)| \end{aligned} \tag{3}$$

With this definition of the stiffener effectiveness metric, the optimization problem for a given loading condition can be defined as:

$$\begin{aligned} &\max_{X_i} M(X_i) \\ &g_j(X_i) \le 0 \end{aligned} \tag{4}$$

where, X_i, are the design variables controlling the shape and end point locations of the stiffeners. Results from a sample problem with 4 stiffeners are shown in Fig. 4. Parametric study of the minumum stiffened panel mass revealed a mild plateau around these optimized locations, suggesting that both configurations existed in the vicinity of the global minima.

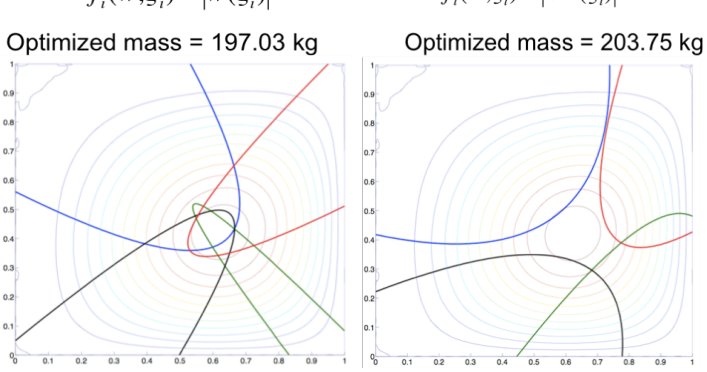

Figure 4: Optimized stiffener location for the sample problem

5. Damage Tolerance Assessment of Curvilinear-Stiffened Unitized Structures

Before unitized structures can be used in the aerospace industry, their damage tolerance behavior will have to be investigated. Here, we outline a framework for damage tolerance assessment and this work is done in a simple crack configuration. The methodology is adapted from Moran, Bordas and Conley [4] on how a damage tolerance analysis of an aerospace structure can be done.

The work starts with a preliminary static strength analysis of the components that enable us to determine stress and strain distributions and to isolate highly stressed, critical regions of the unitized structure (Fig. 6). After that, we set up a sample angled crack configuration ($\theta = -45^o$) with an initial crack length a =12mm at the center of panel for crack propagation analysis. The problem is modeled by shell elements in ABAQUS. We computed fracture parameters such as J-integral, stress intensity factors and energy release rate. We computed stress intensity factors using the domain integral method. Crack propagation direction criterion chosen here is the maximum tangential stress criterion. The maximum tangential stress theory postulates that the crack will begin to grow from its tip in the direction of maximum tangential stress.

Figure 7 shows the evolution of the mode I stress intensity factor with crack length for panel with stiffeners and without stiffeners. No published figures are available for comparison, however it is interesting to note that K1 value decreases for panel with stiffeners, this gives a good prediction. In our current work, we predict the crack growth curve using linear elastic fracture mechanics (LEFM), according to the Paris region.

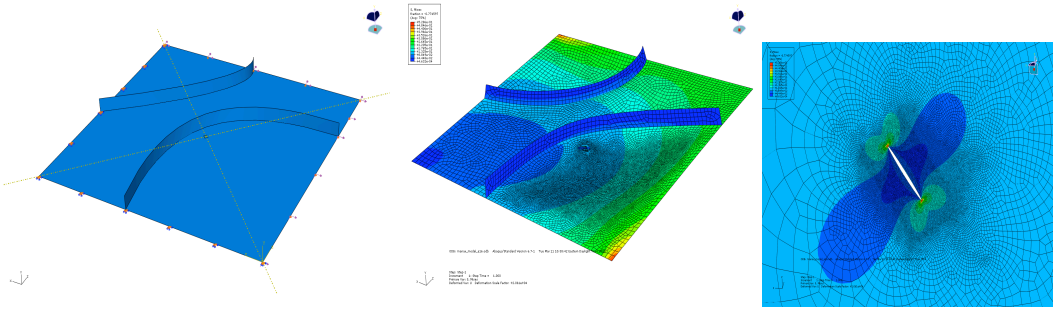

Figure 6: Curvilinear-stiffened unitized structure panel under tension and shear loading, and cracked configuration

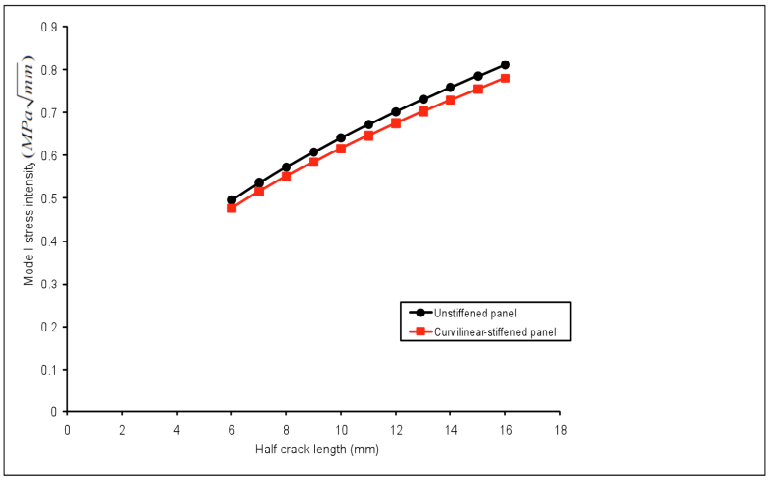

Figure 7: Evolution of the mode I stress intensity factor versus crack length

Acknowledgement

The work presented here was funded by NASA Langley Research Center under a grant administered by the National Institute of Aerospace (Karen Taminger, Grant Monitor) and NASA Subsonic Fixed Wing Hybrid Body Technologies NRA (NASA NN L08AA02C) with Ms. Karen Taminger as the PM and Ms. Cynthina Lach as the COTR. We are thankful to Ms. Taminger and Ms. Lach for their suggestions.

References

[1] Kapania, R. K., Li, J., and Kapoor, H., Optimal Design of Unitized Panels with Curvilinear Stiffeners, AIAA 5th Aviation, Technology, Integration, and Operations Conference (ATIO)/16th Lighter-than-Air and Balloon Systems Conference, 26-28 Sep. 2005, Hyatt Regency Crystal City, Arlington, Virginia.

[2] Mulani, S. B., Li, J., Joshi, P., and Kapania, R. K., Optimization of Stiffened Electron Beam Freeform Fabrication (EBF3) panels using Response Surface Approaches, 48th AIAA/ASME/ASCHE/AHS/ASC Structures, Structural Dynamics Materials Conference, 23-26 April 2007, Honolulu, Hawaii, AIAA 2007-1901.

[3] Queipo, N. V., Haftka, R. T., Shyy, W., Goel, T., Vaidyanathan, R., and Tucker, P. K., Surrogate-Based Analysis and Optimization, *Progress in Aerospace Sciences*, Vol. 41, 2005, pp. 1-28.

[4] Moran, B., Bordas, S., and Conley, J., Damage Tolerance Assessment of Complex Aerospace Structures, Design and Quality Assurance Premium Quality Aerospace Castings, FAA Contract DTFA 03-98-FIA025, Northwestern University, Center for Quality Engineering and Failure Prevention. 2003

Proceedings of the 6th International Conference on
Computation of Shell and Spatial Structures
IASS-IACM 2008: "Spanning Nano to Mega"
28-31 May 2008, Cornell University, Ithaca, NY, USA
John F. ABEL and J. Robert COOKE (eds.)

Buckling analysis of Wuhan Railway Station

TANG Rongwei *, ZHAO Pengfei, TAO Yong, PAN Guohua, QIAN Jihong, DU Yixin

*China Academy of Building Research.
No 30 Beisanhuandonglu, Beijing100013, China
E-mail: tangrongwei@cabrtech.com

Abstract

Wuhan Railway Station Roof is composed of central roof, north wing roof and south wing roof, and the total roof area is about 143000m^2, with the plane dimension 310m×470m. The main support system of the central roof is composed of five main arches with the maximum span of 116 meters, five second arches, and leaned columns. Such support system is called "arch- shell combined system" in this paper. In order to study the stability behavior of the "arch-shell combined system", four cases of buckling analysis are done. And the results show that the shell plays an important role in preventing the buckling of the arch.

1. Introduction

Wuhan Railway Station Roof is composed of central roof, north wing roof and south wing roof, and the total roof area is about 143000m2, with the plane dimension 310m×470m.

The shape of the central roof is like a crane (Fig.1), and the main support system of the central roof is composed of five main arches with the maximum span of 116 meters, five second arches, and leaned columns (fig.2). The distance between theses arches is 64.5 meters, and in the head part of the crane, the cantilever span is about 30 meters. Above the arches, there is a two-layered lattice shell structure. It should be pointed out that the shell supported by arch not directly, but by V branches. We call the combined structure as "arch- shell combined system". The sections of main arches and half arches are variable steel circle sections and the tube directly welded joint is adopted in roof lattice shell.

In order to investigate the stability behavior of such an "arch- shell combined system" deeply, four cases of buckling analysis are done which will be illustrated detailed in following parts.

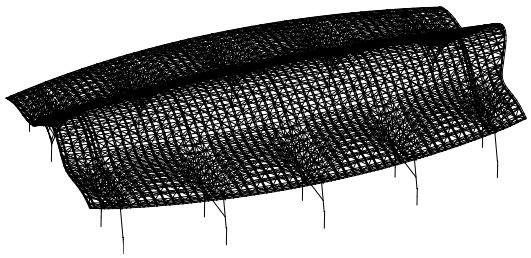

Figure 1 the central roof of wuhan railway station

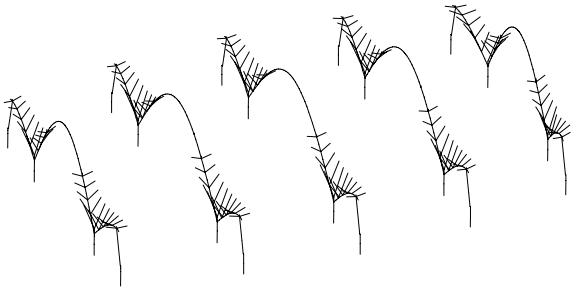

Figure 2 the support system of the central roof

2. Buckling Analysis

2.1 Case 1

In order to study the stability behavior of the main arch, the buckling analysis is performed on the main arch only, and a vertical load of 1kN is applied on every node of the main arche (Fig.3). the load condition of the next three cases are same as case 1. So the the results can be compared easily. The DOF of out-plane is

constrained, because in such an arch-shell combine system the stability of out-plane are strong than in-plane which will be find in case 4. The results(Fig.3) shows that the first bucking modal is asymmetric, and the second buckling modal is symmetric. The buckling factor(show in the bracket) is very low.

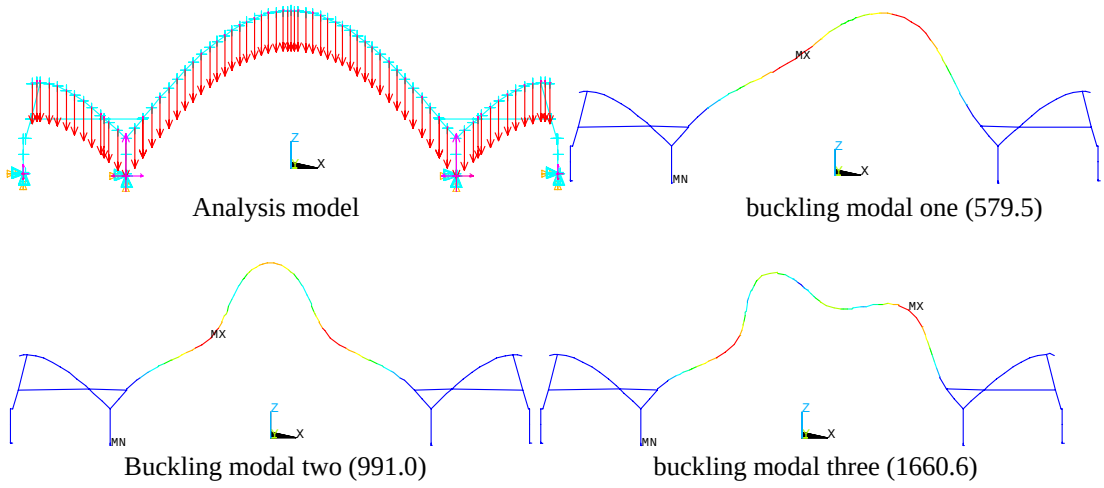

Figure.3 case1 buckling mode

2.2 case 2

In this case, addition to the main arch, only the truss just above the arch is taken into account, and the aim of this case is to investigate how the stiffness of the middle part of the arch affects the stability of the arch. and also the DOF of out-plane is constrained. The results(Figure.4) shows that the first three buckling modal shapes are almost indentical to case 1, but the buckling factor is almost 2 times of the case 1. So it can easily be concluded that the siffness of the middle part of the arch play an important role in the stability behavior of the arch.

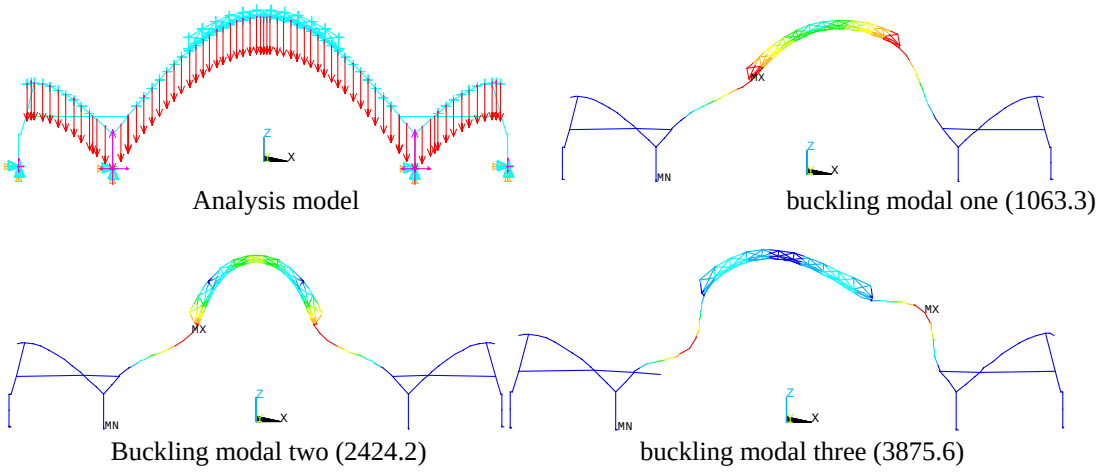

Fig.4 case1 buckling mode

2.3 case 3

In this case, the stiffness of the three piece of struss of the shell near the arch is considered. The truss is connected to main arch and second arch by V branches. The results(Figure.5) shows that the buckling factor is much bigger than case 1 and case 2. also the buckling modal shape are different from previous cases. For the struss connects the main arch and second arch tightly and the foot of the main arch, second arch and the truss composed a very strong triangle structrue(Figure.6), the middle part of the arch buckles fisrt.

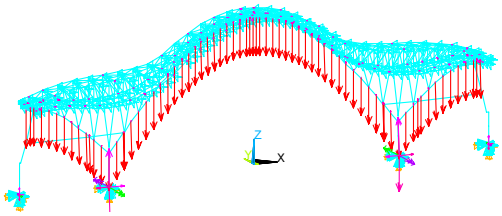

Analysis model

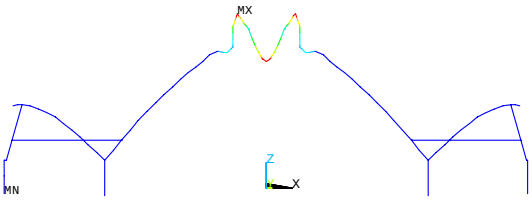

buckling modal one (5475.9)

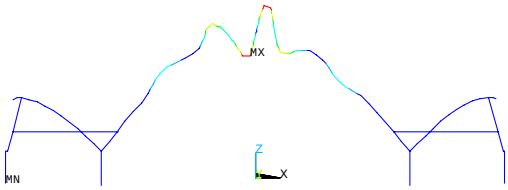

Buckling modal two (7781.5)

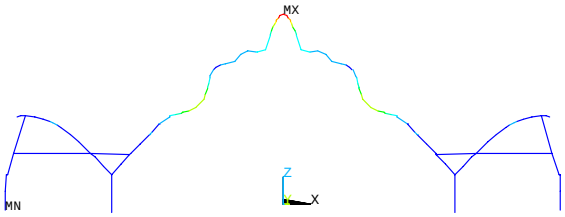

buckling modal three (8888.4)

Figure.5 case1 buckling mode

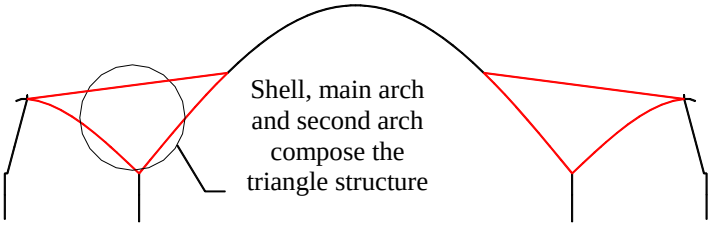

Figure.6 triangle structure

2.4 case 4

In this case, the whole structure is considered, that is to say that the whole contribution of the shell is considered. The results(Figure.7) shows that the buckling factors of the first three modal is a little bigger than case 3, and the modal shapes are almost identical to case 3. Results also show that the buckling of in-plan is prior to buckling of out-plan, that is why in the first three cases the DOF of out-plane is constrained.

Table 1 shows the first ten buckling factors of these four cases.

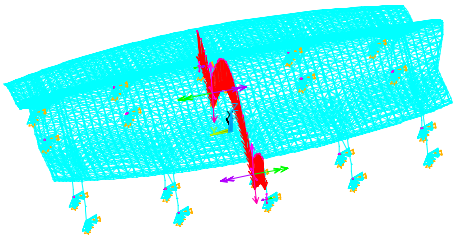

Analysis model

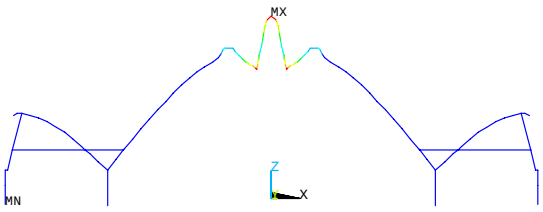

buckling modal one (6030.5)

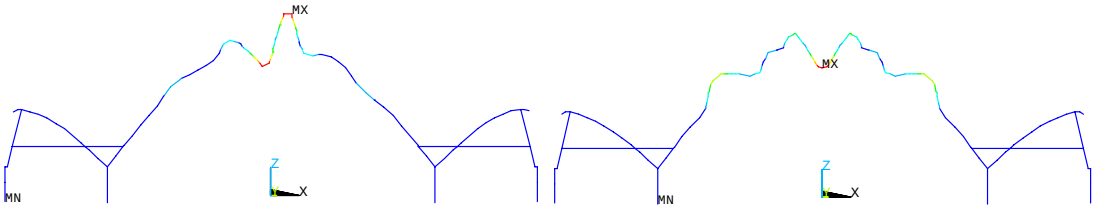

Buckling modal two (8625.7) buckling modal three (9706.2)

Figure.7 case 4 buckling mode

Table 1 compare of the buckling factors of the four cases

mode	Case 1	Case 2	Case 3	Case 4
1	579.7	1063.3	5475.9	6030.5
2	991.0	2424.2	7781.5	8625.7
3	1660.6	3875.6	8888.4	9706.2
4	2442.4	4068.8	9378.1	10339.0
5	3378.8	7877.8	9574.7	11511.0
6	4131.8	9083.5	9633.3	11687.0
7	5216.3	9804.7	9827.8	11688.0
8	6515.0	13139.0	10059.0	12076.0
9	8094.8	14655.0	11059.0	12090.0
10	9445.8	14660.0	11070.0	12411.0

3. Conclusion

From the above buckling analysis, some conclusions can be obtained:

First, for such an “arch-shell combined system”, the shell plays a very important role in preventing the buckling of the arch, and the stability behavior of the arch-shell combined system will be severely under-estimated if the shell is not considered.

Second, for such an “arch-shell combined system”, the out-plan stability is usually superior to the in-plan stability just because the shell connected these arches tightly.

Third, during the preliminary design period, it is a reasonable method to just consider some pieces of the shell above the arch to investigate the stability behavior of the arch-shell combined system.

References

[1] Timoshemko, S.P.and Gere, J.M. Theory of Elastic Stability, 2nd. Ed. McGraw-Hill, 1961.

[2] Bleich.F.Buckling Strength of Metal Structures. McGraw-Hill, 1952.